GEORG-AUGUST-UNIVERSITÄT GÖTTINGEN IN PUBLICA COMMODA SEIT 1737

UNIVERSITÄT FÜR BODENKULTUR WIEN
University of Natural Resources and Life Sciences, Vienna

Master Thesis

Soil Carbon Dioxide Fluxes from Two Austrian Forests under Drying Rewetting Stress

submitted by

Franco Alexis GONZÁLEZ

In the framework of the Master programme

International Master in Soils and Global Change (IMSOGLO)

in partial fulfilment of the requirements for the academic degree

Master of Science

Vienna, August 2022

Co-supervisor:
Univ. Prof. Dr Alexander Knohl
Centre of Biodiversity and Sustainable Land Use (CBL)
Department of Bioclimatology,
Faculty of Forest Sciences,
Georg-August-Universität, Göttingen, Germany

Supervisor:
Univ. Prof. DI Dr. Sophie Zechmeister-Boltenstern
Institute of Soil Research
Department of Forest and Soil Sciences,
University of Natural Resources and Life Sciences,
Vienna, Austria

Master Thesis

Soil Carbon Dioxide Fluxes from Two Austrian Forests under Drying Rewetting Stress

Submitted by

Franco Alexis González

In the framework of the

International Master of Science in Soils and Global Change (IMSOGLO)

in partial fulfilment of the requirements for the academic degree

Master of Science

Vienna, July 2022

Main Supervisor:
Univ. Prof. Dr Phil. Sophie Zechmeister-Boltenstern
Institute of Soil Research
Department of Forest and Soil Sciences
University of Natural Resources and Life Sciences Vienna

Co-Supervisors:
Dr Eugenio Diaz-Pines
Institute of Soil Research
Department of Forest and Soil Sciences.
University of Natural Resources and Life Sciences Vienna

MSc. Dylan Goff
Institute of Soil Research
Department of Forest and Soil Sciences.
University of Natural Resources and Life Sciences Vienna

Univ. Prof. Dr Alexander Knohl
Centre for Biodiversity and Sustainable Land Use (CBL)
Department of Bioclimatology
Faculty of Forest Sciences
Georg-August-Universität Göttingen

Affidavit

I hereby declare that I have authored this master thesis independently, and that I have not used any assistance other than that which is permitted. The work contained herein is my own except where explicitly stated otherwise. All ideas taken in wording or in basic content from unpublished sources or from published literature are duly identified and cited, and the precise references included.

I further declare that this master thesis has not been submitted, in whole or in part, in the same or a similar form, to any other educational institution as part of the requirements for an academic degree.

I hereby confirm that I am familiar with the standards of Scientific Integrity and with the guidelines of Good Scientific Practice, and that this work fully complies with these standards and guidelines.

Vienna, August 15th Franco Alexis GONZÁLEZ *(manu propria)*

Acknowledgements

I want to thank the moral support of my partner, who became my wife during this motivating and challenging journey. I also felt the support of my family and friends in Buenos Aires, sending from abroad the best of their wishes and expectations.

I am very grateful to my supervisors, Eugenio Díaz-Pinés, Dylan Goff, Sophie Zechmeister, and Alexander Knohl, for their guidance, support, and patience during the Thesis Project. I also thank Barbara Kitzler for helping in the field and providing vital field data (BFW).

To the fabulous people, my IMSOGLO colleagues, with who I got the opportunity to share unforgettable moments during this vital process of our lives. I wish all of them the best of success in their life projects.

To the IMSOGLO team and professors for all their crucial contributions to this educational project.

To the ERASMUS MUNDUS project for their financial support on this life-changing experience.

To my colleagues at the Edaphology Chair at the Faculty of Agronomy from Buenos University for their support and for encouraging me to apply and take this opportunity.

Table of content

Affidavit i
Acknowledgements ii
Table of content iii
Abstract v
Kurzfassung vi
1. Introduction 1
1.1. Anthropogenic climate warming and its impacts 1
1.2. Land and soil carbon cycle 2
1.3. The nature of soils and their contribution to climate warming 3
1.4. Rs drivers 3
1.4.1. Soil temperature 3
1.4.2. Soil moisture 4
1.5. Effect of DRW cycles on soil and Rs 4
1.5.1. Drought 4
1.5.2. Rewetting and “Birch effect” 5
1.6. Other drivers of Rs - Spatial variability 6
1.7. Atmospheric N deposition effect on soil CO_2 efflux 6
1.8. Objectives 7
1.9. Hypothesis 7
2. Materials & Methods 8
2.1. Experimental Site 8
2.2. Timespan and experimental design 8
2.3. Rainfall manipulation 9
2.4. N fertilization 10
2.5. Soil CO_2 flux estimation 11
2.5.1. Flux calculation 11
2.6. Soil sampling 12
2.6.1. Laboratory analysis 12
2.7. Meteorological data 13
2.8. Data handling and statistical analysis 14
3. Results 16
3.1. Spatial variability 16
3.2. Temporal variability 18

3.3. Meteorological data 20
3.4. Regression analysis 21
3.5. Contour plots 22
4. Discussion 25
5. Conclusions 28
References 29
List of tables / figures 38
Appendix A: Supplementary data 1

Abstract

More frequent and severe extreme weather and climate events are among the outcomes of global warming. Hence, more frequent and intense dry-rewetting (DRW) stress is expected. Soils play an essential role in controlling GHGs' atmospheric concentration, not only by direct emissions after the turnover of elements but also by sequestering vast amounts of C. Soil organic carbon (SOC) is the largest terrestrial C pool, estimated at around 1700 Pg C, roughly thrice and twice as big as the vegetation and the atmospheric pool, respectively. Rs, performed by microorganisms and plant roots, releases vast amounts of CO_2 (~94 Pg C yr^{-1}), representing the largest C flux between land and the atmosphere after photosynthesis and being almost ten times higher than fossil fuel emissions on an annual basis. Soil temperature and moisture are primarily known to control Rs temporal variability, although other soil parameters that regulate microbial activity can also be important when spatial variability is considered. A prolonged period without water input dries the soil below the field capacity, modifying several physical and biological processes. Rewetting dry soils usually triggers a disproportionated burst of CO_2, a phenomenon known as the "Birch effect", that would be decoupled from microbial growth. Twentieth-century industrial fixation of N_2 into reactive N (Nr) forms for posterior release in ecosystems resulted in a "cascade" of intended and unintended consequences for the C cycle still unclear. Among several effects, the increased Nr over temperate forests has been generally described as reducing Rs and increasing C sequestration. This study aims to assess the effect of drying-rewetting stress on the soil CO_2 fluxes and to uncover the controlling soil parameters in one mature European beech (Fagus sylvatica L.) forest in Eastern Austria during one drying-rewetting stress event, under different nitrogen deposition scenarios.

Kurzfassung

Häufigere und heftigere extreme Wetter- und Klimaereignisse gehören zu den Folgen der globalen Erwärmung. Daher wird ein häufigerer und intensiverer Dry-Rewetting (DRW)-Stress erwartet. Böden spielen eine wesentliche Rolle bei der Kontrolle der atmosphärischen Konzentration von Treibhausgasen, nicht nur durch direkte Emissionen nach dem Umsatz von Elementen, sondern auch durch die Bindung großer Mengen an C. Der organische Kohlenstoff im Boden (SOC) ist der höchste terrestrische C-Speicher, der auf etwa 1700 Pg C geschätzt wird , ungefähr dreimal und doppelt so groß wie die Vegetation bzw. der atmosphärische Pool. Rs, die von Mikroorganismen und Pflanzenwurzeln durchgeführt wird, setzt riesige Mengen an CO_2 (~94 Pg C pro Jahr) frei, was den größten C-Fluss zwischen Land und Atmosphäre nach der Photosynthese darstellt und fast zehnmal höher ist als die jährlichen Emissionen aus fossilen Brennstoffen . Es ist in erster Linie bekannt, dass Bodentemperatur und Feuchtigkeit die zeitliche Variabilität von Rs steuern, obwohl andere Bodenparameter, die die mikrobielle Aktivität regulieren, auch wichtig sein können, wenn die räumliche Variabilität berücksichtigt wird. Ein längerer Zeitraum ohne Wasserzufuhr trocknet den Boden unterhalb der Feldkapazität aus, wodurch mehrere physikalische und biologische Prozesse modifiziert werden. Die Wiedervernässung trockener Böden löst in der Regel einen überproportionalen CO_2-Ausstoß aus, ein als „Birkeneffekt“ bekanntes Phänomen, das vom mikrobiellen Wachstum entkoppelt wäre. Die industrielle Fixierung von N2 in reaktive N(Nr)-Formen im 20. Jahrhundert zur späteren Freisetzung in Ökosystemen führte zu einer „Kaskade“ beabsichtigter und unbeabsichtigter Folgen für den C-Kreislauf, die noch unklar sind. Neben mehreren Effekten wurde die erhöhte Nr. über Wäldern der gemäßigten Breiten allgemein als Verringerung von Rs und Erhöhung der C-Sequestrierung beschrieben. Diese Studie zielt darauf ab, die Wirkung von Trocknungs-Wiedervernässungs-Stress auf die CO_2-Flüsse im Boden zu bewerten und die kontrollierenden Bodenparameter in einem ausgewachsenen Rotbuchenwald (Fagus sylvatica L.) in Ostösterreich während eines Trocknungs-Wiedervernässungs-Stressereignisses unter verschiedenen Stickstoffbedingungen aufzudecken Ablagerungsszenarien.

1. Introduction

1.1. Anthropogenic climate warming and its impacts

Anthropic activity is warming the global surface by enhancing the atmospheric greenhouse effect (IPCC, 2013). The greenhouse gas (GHG) concentration sharply augmented over the last two and a half centuries (ca. 1750; IPCC, 2013), which is attributed to the skyrocketed human-derived emissions of the three main gases, carbon dioxide (CO_2), nitrous oxide (N_2O), and methane (CH_4). After water vapour, the main contributor to the greenhouse effect is CO_2, and its atmospheric concentration rose from ~277 ppm from 1750 to ~414 in 2021 (Friedlingstein et al., 2022). Fossil fuel combustion is the largest source, followed by land use and land cover change (LULCC). Humans have burned ~450 Pg C since 1870 (Le Quéré et al., 2018, Friedlingstein et al., 2021). Likewise, LULCC contributes to GHGs emissions directly by disrupting large C pools (e.g., deforestation) or indirectly by reducing the terrestrial ecosystem's sink capacity, such as soil C sequestration. The area of land dedicated to pasture and crops has risen from an area between 7.5 to 9 million Km^2 in 1750 to 50 million Km^2 in 2011 (Ciais et al., 2013). Consequently, the resultant total anthropogenic emissions released is 700 ± 75 Pg C for the period 1750-2019, from which fossil fuels contributed 64% ± 15%, and the remaining arose from LULCC (Arias et al., 2021), and most of these emissions occurred after 1960 (~70%; Friedlingstein et al., 2021). There has been a strong increasing tendency in anthropogenic-derived CO_2 emissions in the last six decades, reaching its highest levels in the decade 2010-2019, with an average annual value at 10.9 ± 0.9 Pg C y^{-1}, which 46% of it ending at the atmosphere while 31% was retained by terrestrial ecosystems (land-borne fraction; Friedlingstein et al., 2021) and the oceans mainly absorbed the remaining. The increase was exclusively due to fossil fuel emissions which have risen from 3 to ~10 Pg C yr^{-1} from 1960 to 2021, while LULCC decreased from 1.6 to 0.8 Pg C yr^{-1} (Friedlingstein et al., 2021). The land C sink is expected to increase in magnitude with higher atmospheric CO_2 levels, but the share of the emissions captured will decrease, and a warmer and dryer climate will slow the growing sink effect (Arias et al., 2021). As a result, the human warming effect is estimated on 1.09 (0.95-1.20) °C since the 1850-1900 baseline, and it will cross the 1.5 °C level soon (2030-2052; Arias et al., 2021) with important already unavoidable negative consequences for earth ecosystems in the present century no matter the course of actions (e.g., emission reduction), and further catastrophic predictions for the next centuries if emissions do not strongly decline.

More frequent and severe extreme weather and climate events are among the outcomes of global warming (Sherwood & Fu, 2014). Since 1950 there has been good observational proof confirming an increase in frequency and heavy precipitation over most land regions (Arias et al., 2021; Hartman et al., 2013). This would lead to less water available since when the water input exceeds the soil retention capacity, it is not incorporated into the soil and flows away as runoff or deep percolation. Similarly, heatwaves and droughts were more frequent in the last century and are expected to increase alongside global warming (Orth et al., 2016); both types of events also deplete soil water availability due to enhanced evapotranspiration. Hence, more frequent and intense dry-rewetting (DRW) stress is expected.

1.2. Land and soil carbon cycle

Soils play an essential role in controlling GHGs' atmospheric concentration, not only by direct emissions after the turnover of elements but also by sequestering vast amounts of C. Terrestrial plant photosynthesis, termed gross primary production (GPP), removes CO_2 from the atmosphere at a rate estimated between 119 and 169 Pg C yr^{-1} (Anav et al., 2015), which represents roughly one out of eight atmospheric CO_2 molecules (Reich, 2010) and the major land C sink. GPP mainly depends on the vegetation-growing season (Goulden et al., 1996). Although most of this C is reemitted to the atmosphere by respiration (mainly from soils), the share of C in dead material deposited over soils which is not fully degraded and mineralised back to CO_2 interacts with mineral soil particles (Rasmussen et al., 2018), and gradually builds up the soil organic matter (SOM), which is a pool with much higher residence times (centuries; Ciais et al., 2013). The degradation rate of litter depends on several factors, which in turn are mainly controlled by vegetation species, such as the litter quality (e.g., C, N, cellulose, and lignin contents) and quantity, the microbial community of decomposers, carbohydrate allocation, root biomass and surface soil temperature and moisture (Fernández-Alonso et al., 2018a). In particular, litter in beech forests is rich in lignin and cellulose content, and hence fungi dominate the microbial community because they can better use that substrate than bacteria (Schneider et al., 2012). However, once inside the soil, the interaction between SOM and small particles (clay; <2 μm) surfaces is complex and partially understood (Rasmussen et al., 2018). In general, more clay content gives more physical protection to SOM, promoting stabilisation and preventing C depletion (Hartley et al., 2021), but also the chemical composition of the SOM plays a role (Conant et al., 2011). Moreover, the van Bemmelen factor assumes that more than half of SOM is C (i.e. 58%; Howard & Howard, 1990). This soil organic carbon (SOC) is the largest terrestrial C pool, estimated at around 1700 Pg C, roughly thrice and twice as big as the vegetation and the atmospheric pool, respectively (Canadell et al., 2022). Likewise, global forests act as permanent net sinks of C, e.g. Pan et al. (2011) estimated a sink effect of temperate forests of 0.78 ± 0.09 Pg C yr^{-1} for the period 2000-2007.

Climate change's impact on the land sink, and SOC, will depend on the future atmospheric CO_2 concentration scenarios. On the one hand, the land C sink is expected to increase with the atmospheric CO_2 concentration (fertilisation effect; Friedlingstein et al., 2021), which can lead to more SOC. However, the sequestration effect of land and soils can be reversed in the potential (and desired) scenario of decreased atmospheric CO_2 (Friedlingstein et al., 2021). On the other side, global warming enhances GPP (more C input) but also soil respiration (R_s) (Bond-Lamberty & Thomson, 2010), where there is no water limitation. Furthermore, the SOC decrease effect due to warming might be lower for fine-textured soils (clay protection effect; Hartley et al., 2021). Likewise, soil moisture content variability reduces the land C sink (Green et al., 2019). Nevertheless, the net effect of global warming on SOC is not clear yet (Davidson & Janssens, 2006; van Gestel et al., 2018), and the same applies to more frequent and intense droughts (Canadell et al., 2022). In addition, increased nitrogen deposition can increase C fixation in temperate forests ecosystems (see section 1.7), although it would be less important compared with CO_2 fertilisation and climate change effects (e.g., precipitation and temperature patterns changes; Zaehle & Dalmonech, 2011; Ciais et al., 2013; Fernández-Alonso et al., 2021).

R_s, performed by microorganisms and plant roots, releases vast amounts of CO_2 (~94 Pg C yr^{-1}), representing the largest C flux between land and the atmosphere after photosynthesis (Xu & Shang, 2016) and being almost ten times higher than fossil fuel emissions on an annual basis (Canadell et al., 2022). Part of the SOC is partially protected by complexation with clay-sized minerals or by aggregates occlusion (Hartley et al., 2021). However, microbes rapidly decompose the accessible part of SOC (Schimdt et al., 2011) and litter while plants roots respire photosynthates, and both processes combined conform the soil respiration, and this is the main origin of the soil CO_2 efflux (Chemical oxidation and carbonate dissolution also exist; Lankreijer et al., 2003). Moreover, Rs represents between 60-80% of ecosystem respiration in temperate broad-leaved forests (Granier et al., 2003).

1.3. The nature of soils and their contribution to climate warming

The soil is a complex three-dimensional entity which consists of mineral and organic materials of varied sizes and chemical compositions. The finer the material and the more SOM content, the higher the ability to agglutinate and form porous corps, known as soil macro and micro aggregates (Six et al., 2004). The granular size composition, termed soil texture, together with the aggregation capacity, leads to the spatial arrangement of pores, termed soil structure, which defines essential soil functions like water holding or air capacity (Cosby et al., 1984; Moyano et al., 2013), both regulators of the biochemical reactions. Soil structure varies among different types of soils (e.g., agricultural vs forest soils) and soil horizons (e.g., superficial vs non-superficial), and so do the processes that depend on it. Furthermore, SOM association with clay-minerals to form microaggregates prevents its mineralization (Six et al., 2004).

1.4. R_s drivers

Soil temperature and moisture are primarily known to control R_s temporal variability (Davidson et al., 2006a; Bahn et al., 2009 & 2010), although other soil parameters that regulate microbial activity can also be important when spatial variability is considered. Soil temperature explains most of the temporal variation but only when soil moisture is not too scarce or too abundant (Valentini et al., 2003; Bahn et al., 2010; Leitner et al., 2017; Fernández-Alonso et al., 2018b; Moyano et al., 2013).

1.4.1. Soil temperature

Microbial and plant roots activities are especially sensitive to temperature changes, usually showing a positive correlation (Janssens et al., 2003). Several equations have been used to describe the CO_2 relationship against temperature, as summarised in Janssens et al. (2003), who support the Arrhenius-type equation best describes the Rs-temperature relation. Other equations are linear, power, sigmoid, and exponential. The exponential equation Q_{10} is often used, but the authors criticised it since it underestimated fluxes at low temperatures and overestimated them at high temperatures (Lloyd & Taylor, 1994). However, their fitting exercises showed that both Arrhenius and Q_{10} relationships overestimated fluxes at high

temperatures from summer and, most importantly, coincided with lower soil moisture content. However, the performance of the models substantially improves when incorporating the moisture factor. Because of this, the authors highlighted the importance of manipulative experimentation (water exclusion and irrigation) under dry and warm conditions in the summer period to explore soil moisture scenarios that would be carried out later more extensively (e.g., Almagro et al., 2009; Bahn et al., 2010; Leitner et al., 2017; Fernández-Alonso et al., 2018 & 2021).

1.4.2. Soil moisture

Soil moisture is the main factor explaining soil CO_2 efflux when it is scarce. This has been described for several forests' ecosystems (Epron et al., 1999; Curiel Yuste et al., 2003; Almagro et al., 2008; Luo et al., 2012; Leitner et al., 2017; Fernández-Alonso et al., 2018). Moreover, an exacerbated reaction has been described when the soil water content is recovered after a dry period (Almagro et al., 2008; Birch, 1958; Curiel Yuste et al., 2003 & 2007; Fierer & Schimel, 2002; Jarvis et al., 2007; Miller et al., 2005; Orchad & Cook, 1983; Xiang et al., 2008), sometimes leading to higher soil CO_2 release compared with continued moisture conditions. This, combined with the projection of an increase in frequency and intensity of DRW events, would positively feedback climate change.

1.5. Effect of DRW cycles on soil and R_s

1.5.1. Drought

A prolonged period without water input dries the soil below the field capacity, modifying several physical and biological processes.

While water film gets disconnected, it reduces the nutrient transport (Skopp et al., 1990), isolating and concentrating the nutrients in smaller pores. Structure stability declines in coarser textures while increases in finer soils. Besides, the extent of shrinking provoked by drying depends on the type and amount of clay. Also, Bimüller et al. (2014) reported a hindered soil N processing (i. e., mineralisation) and posterior stabilisation in organo-mineral fractions during drought, with the potential risk of loss of labile N in extreme rainfall events.

Extremely dry conditions trigger soil microbiota's specific reactions (Borken & Matzner, 2009; Barnard et al., 2020). CO_2 fluxes are highly reduced during dry conditions (Orchad & Cook, 1983; Schimel et al., 1999; Howard & Howard, 1993). The decrease in microbial activity might explain this, and even death, caused by limited water availability (De Nobili et al., 2006). One of the strategies to avoid death by desiccation is concentrating osmolytes (Harris, 1981). Sometimes, forming spores and undergoing dormancy is a better survival strategy. Exudated enzymes maintain active mineralising C and N during drought (Manzoni et al., 2014). The longer the drought period, the greater the impact on the microbial biomass (Schimel et al., 1999), and any resistance strategy represents a cost in energy and nutrients (Schimel et al.,

2007). Lastly, drought promotes hydrophobicity, but Manzoni et al. (2014) considered it and the aggregate stability less important than osmotic regulation and nutrient diffusion for their impact on microbial activity.

1.5.2. Rewetting and "Birch effect"

Rewetting dry soils usually triggers a disproportionated burst of CO_2, a phenomenon known as the "Birch effect" (Jarvis et al., 2007), that would be decoupled from microbial growth (Göransson et al., 2013; Iovieno and Bååth, 2008). Any considerable amount of water addition changes the water potential and has more complex effects than just refilling the soil. The microbial activity recovers sharply after a substantial rewetting, often more than expected in the hypothetical situation of continuous moist soil (Birch, 1958a and b; Fierer & Schimel, 2002; Iovieno and Bååth, 2008; Orchad & Cook, 1983). Recovery after rewetting can take minutes (Borken et al., 2003), but it can also be delayed by dormancy, from 1 to 72 hours (Placella et al., 2012). The delay depends on the drought length (Barnard et al., 2015; Göransson et al., 2013) and harshness (Meisner et al., 2017), the adaptation of microbes to DRW stress (Meisner et al., 2015), and the history of past DRW events with the possible adaptation of microbiota after repeated cycles (Fierer & Schimel, 2002; Leizeaga et al., 2021 & 2022).

Researchers proposed different mechanisms to explain the "Birch effect" (Barnard et al., 2020; Borken & Matzner, 2009; Evans et al., 2006; Fierer & Schimel, 2003; Manzoni et al., 2014). Microbes need to release the osmolytes accumulated during dry conditions (e.g. proline) the faster as possible to avoid plasmolysis, and these components would be quickly mineralised. However, because the turnover time is short (Warren, 2019), it is hard to demonstrate that released osmolytes actually provide a source of C. Hence, contradictory results exist (Boot et al., 2013; Warren, 2014; Williams & Xia, 2009). Microbial death, either by plasmolysis (Kief et al., 1987) or infection by phages and viruses (Williamson et al., 2017), also might contribute as C source. Water film disconnection due to dryness promotes microbial diversity (Carson et al., 2010), which provides higher adaptability and possibly faster recovery when the porosity film connection returns. The persistence of activated exoenzymes is another proposed explanation (Lawrence et al., 2009). However, Homyak et al. (2018) did not find evidence of persistent exoenzyme activity in dry soils. Clay complexes can release organic matter by desorption (Blankinship & Schimel, 2018). The disruption of aggregates releases occluded organic matter (Cosentino et al., 2006), which would also be an extra C substrate upon rewetting (Navarro-García et al., 2011). When DRW stress releases previously unavailable labile organic compounds (Schimel et al., 2011), the pulse of CO_2 is higher than in continually moist soil (Borken & Matzner, 2009). Nevertheless, the exact mechanistic processes of the DRW cycles are still under debate, and hence also, its effects and interactions with climate change. Furthermore, manipulative field experiments that simulate DRW cycles in temperate forests are lacking.

1.6. Other drivers of R_s - Spatial variability

R_s also shows large spatial variability even within short distances, especially under forest (Bahn et al., 2008; Curiel Yuste et al., 2004; Epron et al., 2004b; Kang et al., 2003; Law et al., 2001; Søe & Buchmann, 2005; Vincent et al., 2006), which can be higher than temporal variability (at least than diurnal variation; Janssens et al., 1998; Law et al., 2001; Rayment & Jarvis, 2000), and can be explained by several soil parameters. As discussed above, soil temperature and moisture are strong predictors of temporal variations, but the explanation of spatial heterogeneity in fluxes might require including other soil parameters. Among those factors, Vincent et al. (2006) have mentioned vegetation (Law et al., 2001) and its roots properties (Janssens et al., 1998), organic matter quantity and quality (Epron et al., 2004b; Rayment & Jarvis, 2000), microbial biomass (Lee & Jose, 2003), and soil texture and the related porosity (Dilustro et al., 2005; Moyano et al., 2012). Furthermore, soil chemistry has also been found to explain R_s in temperate forests, and examples are Janssens et al. (2003) and Borken et al. (2002), both reporting negative correlation with C:N ratios, or Vincent et al. (2006) showing correlations with topsoil N content. In addition, Søe & Buchmann (2005) found a positive correlation of R_s with several soil chemistry parameters (C:N and concentrations of C_{tot}, N_{tot}, P, DOC, among others) and soil structure and roots characterisation parameters. Likewise, Kang et al. (2003) reported that CO_2 efflux variability within short distances could be better explained by soil moisture than temperature. However, more attention has been focused on R_s's temporal rather than spatial drivers.

1.7. Atmospheric N deposition effect on soil CO_2 efflux

Twentieth-century industrial fixation of N_2, inert and abundant (80%) in the atmosphere, into reactive N (N_r) forms (ammonia, nitrates, amino acids, proteins, among others) for posterior release in ecosystems resulted in a "cascade" of intended and unintended consequences for the C cycle still unclear (Arias et al., 2021; Sutton et al., 2011). Satisfying N-demand for food production is a positive effect. On the contrary, a harmful example is that higher emissions of NO_x and NH_x derived from human high-temperature combustion processes and gaseous loss from N-enriched ecosystems have increased the atmospheric N_r deposition (Sutton et al., 2011). In Europe, although deposition in oxidised form (NO_x) has peaked in the 1980s and then halved by 2017, it is still 3-4 times higher than 1900 levels, while the value for the reduced form (NH_x) doubles the 1900 levels and it is not expected to decrease by 2050 (Engardt et al., 2017). Among several effects, the increased N_r over temperate forests has been generally described as reducing R_s and increasing C sequestration (Dirnböck et al., 2017; Janssens et al., 2010; Pregitzer et al., 2008; Zhou et al., 2014; Zhong et al., 2016), with the magnitude moderated by soil conditions, such as previous N_r availability (Dirnböck et al., 2017), or MBC, SOC, bulk density, and pH (Zhong et al., 2016). While dry conditions can also reduce R_s, hampering microbial activity by water limitation (Fernández-Alonso et al., 2021), the interaction between chronic atmospheric N_r deposition under more intense and frequent DRW cycles has not been adequately assessed yet.

1.8. Objectives

This study aims to assess the effect of drying-rewetting stress on the soil CO_2 fluxes and to uncover the controlling soil parameters in one mature European beech (Fagus sylvatica L.) forest in Eastern Austria during one drying-rewetting stress event, under different nitrogen deposition scenarios.

Specific objectives

a) We will assess whether potential future intensified summer DRW stress in temperate forests enhances or hampers soil CO_2 efflux.
b) We will describe the effect of increased atmospheric N_r deposition on the soil CO_2 efflux under DRW stress.
c) Exploring the explanatory power of soil parameters will improve mechanistic understanding of any response of CO_2 efflux to the changing environmental conditions.
d) We will describe the spatial variability of soil CO_2 efflux, identifying possible emission "hot spots".
e) We will try to identify if the "Birch effect" occurs under the specific soil moisture of a temperate forest during a summer drought.

1.9. Hypothesis

i) Since rewetting the dry soil expectedly reactivates the microbial activity, soil CO_2 efflux and MBC would rise after irrigation.
ii) If, upon rewetting, the soil CO_2 efflux gets decoupled from soil moisture, meaning there is an exaggerated reaction considering the soil moisture level, it would be attributed to the Birch effect occurrence.
iii) Soil temperature and moisture are strong predictors of R_s, but the latter may be more important in dry conditions. Consequently, the soil moisture would explain the variability in CO_2 efflux better than soil temperature and positively correlate with the CO_2 efflux in the DRW treatment.
iv) Forests soils show high variability of soil biochemical and physical parameters. If this is the case, CO_2 efflux would also show high spatial variability and correlate with any of the biochemical and physical soil parameters monitored.
v) We expect that enrichment of forest soils with N_r will increase the concentration of mineral forms of N, either NO_3^- or NH_4^+, reduce microbial activity (MBC), and suppress soil CO_2 efflux.

2. Materials & Methods

2.1. Experimental Site

We recovered field data from a "Beech" (*Fagus sylvatica L.*) forest stand in Klausen-Leopoldsdorf. This long-term ecosystem research (LTER) site is managed by Federal Research Centre for Forests, Natural Hazards, and Landscape (BFW), and it includes varied research equipment, such as rain-out shelters and an irrigation system, automated chambers for soil-atmosphere gas exchange measurements, and climatic sensors.

We used a managed homogenous beech stand, 80 years old, located 20 km west of Vienna (48°07' N 16°03' E). Since 2006, it has been part of the LTER Austria network. It is also part of the European Level II Forest Monitoring System in the International Co-operative Programme on Assessment and Monitoring of Air Pollution Effects on Forests (ICP Forests). According to Kitzler et al. (2006), the soils are Dystric Cambisols developed over sandstone (WRB), with a loam-loamy clay texture, and the natural N deposition rate is around 13 kg N ha^{-1} y^{-1}. At the plot's site, the elevation is 500 m a. s. l., the slope is exposed to NNE, and the mean annual temperature and precipitation are 8°C and 728 mm. Bulk density is 0.827 g cm^{-3}. Table 2-1 summarises the essential features of the site.

Table 2-1. Main features of site Klausen-Leopoldsdorf. Data based on Kitzler et al. (2006).

Klausen-Leopoldsdorf	
GPS Coordinates	48°07' N 16°03' E
Elevation (m a.s.l.)	500
Annual mean temperature (°C)	8
Annual mean precipitation (mm)	728
Mean pp on vegetation growing period (mm, 1970-2000)	446
Soil classification (WRB)	Dystric Cambisols over Sandstone
Nitrogen deposition rate (kg N ha^{-1} y^{-1})	13
Hill exposition and inclination	NNE
Soil texture	Loam-Loamy clay

2.2. Timeplan and experimental design

The year 2021 was the first of the 3-years-EXAFOR project, which consisted of field monitoring of soil GHGs fluxes and several other associated parameters under a rainfall exclusion experimentation combined with wet N fertilization at two research forest sites, "Klausen-Leopoldsdorf" and "Rosalia". From April till November, covering the vegetation growing period, 3 complete severe DRW cycles were simulated, each of them consisting of 8 weeks of drought without water inputs interrupted by an irrigation event of 150 mm. Only the time distribution of water inputs and not the natural average total amount was manipulated. The 3 irrigation events approximately sum up to the average precipitation recorded for the vegetation growing season for the years 1970 to 2000 (Table 2-1; Kitzler et al., 2006). At Klausen-Leopolsdorf, the rainfall exclusion started on May 4th and ended on November 16th. However, for the current thesis work, only the data for the 28-days-period between August 19th

and September 15th was explored. This includes the last 6 days of the second drought period, the second irrigation event of August 25th, and 22 days more after the rewetting until September 15th (Figure 2-1).

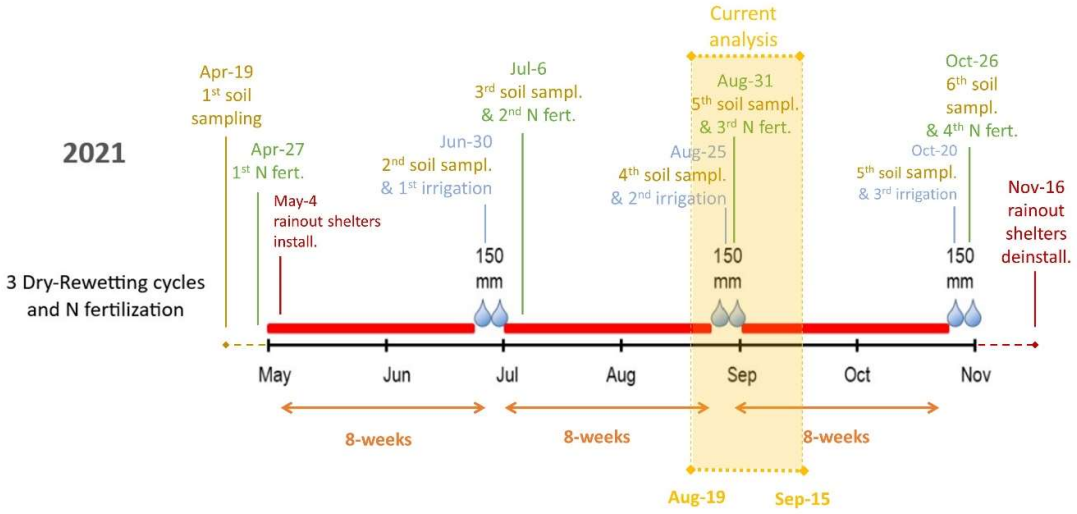

Figure 2-1. Timeplan of the year 2021 at Klausen-Leopoldsdorf research site. Adapted from Institute of Soil Research, BOKU.

The experimental setup included 16 square plots (3x3 m) allocated along a slope (Figure 2-2). The experimental design consisted of a factorial approach, combining two levels of rainfall manipulation (Control and severe DRW stress) with two other N addition scenarios (natural and +50 kg N ha^{-1} a^{-1}). We replicated randomly assigned four plots for each of the four resulting combination treatments ("C", "C + N", "S", and "S + N"). The plots distribution resulted in: Plots number 1, 5, 10, and 13 assigned to "Control" (C) treatment; plots 2, 6, 9, and 14 to "Control with N addition" (C+N); plots 3, 7, 11, and 15 to "Severe DRW stress" (S); plots 4, 8, 12, and 16 to "Severe DRW stress with N addition" (S+N). Consequently, half of the plots were sheltered by May 4th.

2.3. Rainfall manipulation

Rain-out shelters in combination with an irrigation system were used to simulate severe DRW stress in half of the plots (Figure 2-2). The shelters were installed from May 4th till November 16th (Figure 2-1). Appendix A includes photos of the shelters with the irrigation system. At every irrigation event, the volume of water each plot required was:

(0.150m 3m 3m) $plot^{-1}$ = 1.35 m^3 $plot^{-1}$ 1000 L m^{-3} = 1350 L $plot^{-1}$

Which throws a total of:

1350 L $plot^{-1}$ 16 plot = 21600 L

A plastic container bag with a capacity of at least 22 m^3 (22000 L) was placed at a point of the slope of a higher level of all the setup and filled using bombs. Furthermore, the water had to be decalcified to avoid unwanted C and Ca^{2+} inputs to the soil, which could interfere with the

treatments. For that purpose, a descaler system was implemented. The water flowed by the difference in gravitational potential through a flexible line which ended at a 1st transfer 1m^3-container. From the 1st container, the water was pumped to the descaler and then transferred to a second 1m^3 container from which the water was pumped and directed through flexible lines to the irrigation systems mounted at each sheltered plot. Below each shelter, a distribution rigid pipeline system was installed, with a valve and a manometer at the inlet point and water aspersion at several points in the lines. The water pressure was monitored and maintained at a level which allowed homogeneous aspersion over the soil surface.

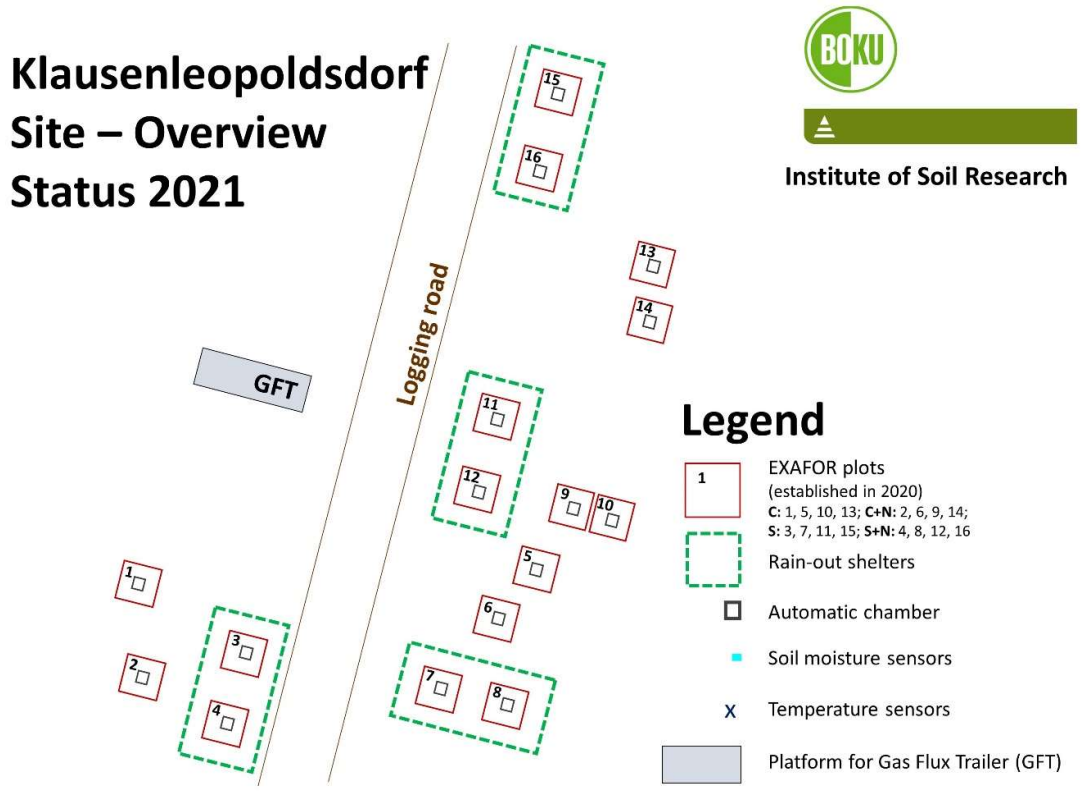

Figure 2-2. Experimental setup at Klausen-Leopoldsdorf research site. Each of the 16 squared plots (3 m x 3 m; red squares), was equiped with an automated chamber (black squares) connected to a "Gas Flux Trailer" (grey rectangle). Half of the plots were covered with rain-out shelters (green dashed rectangles) since May 4th, 2021. The plots were randomly assigned and equally distributed to each of the four treatments resulted. Plots number 1, 5, 10, and 13 were assigned to Control (C) treatment; 2, 6, 9, and 14 to Control with N addition (C+N); 3, 7, 11, and 15 to Severe DRW stress (S); 4, 8, 12, and 16 to Severe DRW stress with N addition (S+N). Source: Institute of Soil Research, BOKU.

2.4. N fertilization

A scenario of increased atmospheric N deposition was simulated by N fertilization in half of the plots at a rate of 50 kg N ha^{-1} y^{-1}. The N addition was subdivided into 4 N fertilization events (Figure 2-1), consisting of 12 kg N ha^{-1}. The amount added at each event for each plot was:

12 kg N ha^{-1} (10000 m^2 ha^{-1})$^{-1}$ = 0.0012 kg N m^{-2}

Multiplied by the area of the plots:

0.0012 kg N m^{-2} (3 m 3 m) $plot^{-1}$ = 0.0108 kg N $plot^{-1}$ = 10.8 g N $plot^{-1}$

A 20 L solution of 0.54 g N L^{-1} concentration was prepared with ammonium nitrate (NH_4NO_3) granular fertilizer and evenly applied in two rounds of 10 L each, with the use of 12 L-capacity backpack sprayers (Appendix A). The addition of 20 L to the plots represented a water input event of:

20 L (1000 L m^{-3})$^{-1}$ (9 m^2)$^{-1}$ = 0.002 m = 2 mm

To compensate for the water applied in the fertilized plots, the unfertilized plots also received an equivalent application of water.

2.5. Soil CO_2 flux estimation

As shown in Figure 2-2, one automated chamber (non-steady-state and non-flow-through; Livingston and Hutchinson, 1995) was placed at the centre of each plot. The chambers used were "black" type because their structure was made of stainless steel, and this material prevents the pass of sunlight, so the light-dependent part of photosynthesis is stopped while the chamber is closed. The chambers were installed over stainless-steel frames inserted 5 cm in the mineral soil, and their dimensions were 0.5 m x 0.5 m (horizontal sides) x 0.15 m (height). Each chamber also contained one fan, which ensures homogeneous air mixing. The 16 chambers were connected to the "GasFluxTrailer", which controlled the opening and closing and the gas sampling timing and contained a cavity-ring-down spectroscope which measures the CO_2 air concentration (Picarro G2301, Santa Clara, USA), among other required equipment (computer, data logger, another spectroscope for measuring N_2O, etc.). The temporal resolution of gas exchange measurements was three hours, while the chamber enclosure time was 10 minutes.

2.5.1. Flux calculation

Once gas concentration inside the chamber is estimated over the 10 minutes enclosure time, the several measured values for the gas concentration inside the chamber combined with the exact measurement time are used to estimate the temporal rate of change of the concentration. This change can be linear or non-linear. Non-linear relations are attributed to artefacts in the chamber technique, but several corrections have been suggested (Parkin & Venterea, 2010). In the case of a constant rate of change, a linear regression can be used to calculate the slope, which would be expressed as, e. g. [µL CO_2-C L^{-1} min^{-1}] or [ppmv min^{-1}]. Due to the relative short enclosure time and large chamber size, the change of rate was calculated with linear regression.

Following Butterbach-Bahl et al. (2011), the steps for the flux of CO_2 [µg C m^{-2} h^{-1}] calculation are:

$$Flux\ of\ CO_2(\mu g\ C\ m^{-2}\ h^{-1}) = \frac{\text{chamber volume}(m^3)\ mol\ weigh\ \ of C(g\ mol^{-1})\ regression\ slope(ppmv\ min^{-1})\ 60\ \text{min}\ 10^6\ \mu g}{chamber\ area\ (m^2)\ mol\ volume\ of\ gas(\ m^3\ mol^{-1})\ hour\ g}$$

But, the molar volume of gas needs to be corrected according to the ideal gas law:

$$mol\ volume\ of\ gas(m^3\ mol^{-1}) = 0.02241\ \frac{(273.15 + Temp(°C))}{273.15}\ \frac{atmospheric\ pressure\ at\ measurement\ height\ (Pa)}{atmospheric\ pressure\ at\ sea\ level\ (Pa)}$$

Atmospheric pressure can be estimated with height above sea level with a barometric formula (Butterbach-Bahl et al., 2011), and headspace air temperature must be measured at the enclosure time.

The unit presented in the current study is mg CO_2-C m^{-2} h^{-1}, hence two more transformations are needed:

mg CO_2-C m^{-2} h^{-1} = µg CO_2-C m^{-2} h^{-1} (10^3 µg mg^{-1})$^{-1}$

Finally, the measurement was done every 3 hours per chamber, but the 8 intraday values were pooled into one daily average.

2.6. Soil sampling

On each sampling date (Figure 2-1), a regular metal mesh of 1.5 m long and 1 m wide, and rectangular cells (5 cm x 5 cm), with columns and rows identified, was placed inside the plots on the right side of the chamber. Five cells defining the soil auger (1 cm diameter) entrance point were randomly selected at each sampling date and discarded for the remaining period. Hence, the auger was introduced 5 times up to 20 cm inside mineral soil after manual litter removal, without repeating the cell in the entire 1-year-campaign. The material recovered inside each auger was divided by depth, from 0-10 and 10-20 cm. The five soil samples from the same depth were pooled, sieved (2 mm) and enclosed in bags. At this point, we weighted each bag (2 per plot) to ensure we contained 20 g of soil at a minimum, and if needed, one extra augering at a random point was performed. In the end, the two bags were adequately closed and refrigerated for posterior transport to the laboratory. This procedure was repeated in the 16 plots.

The current thesis includes the 4th (Aug 25th) and 5th (Aug 31st) soil sampling campaigns (Figure 2-1).

2.6.1. Laboratory analysis

At the lab, we analysed the soil samples to obtain soil texture and moisture and the concentrations of microbial biomass carbon (MBC) and nitrogen (MBN), dissolved organic carbon (DOC), total dissolved nitrogen (TDN), ammonium (NH_4^+), and nitrate (NO_3^-).

By the Chloroform-Extraction-Method (Schinner and Sonnleitner, 1996), we obtained the microbial biomass carbon (MBC) and nitrogen (MBN).

We measured in a carbon and nitrogen total analyser (TOC-L, Shimadzu, Kyoto, Japan) the total dissolved carbon (TDC) and nitrogen (TDN) after extracting with 0.5 M K_2SO_4 solution, 30-min shaking, and N-free filtering. We read NH_4^+ and NO_3^- following Jones and Willett (2006), which also allowed us to estimate dissolved organic nitrogen (DON) by subtraction.

The non-fumigated extract allowed us to estimate the dissolved organic carbon (DOC) and nitrogen (TDN).

Soil texture was obtained by sedimentation; We weighted the samples before and after oven drying (105 °C) to estimate soil moisture content.

2.7. Meteorological data

The Gas Flux trailer has installed a tipping bucket for estimating precipitation and an air temperature sensor located 2 m above ground. Both types of equipment have a temporal resolution of 1 minute.

In addition, BFW provided data for the following parameters: Soil temperature at 5 cm depth, measured with thermocouples; Soil water content estimated by water content reflectometer. The time resolution of this data was 30 min. However, sensors were installed only in 4 plots, 2 sheltered and 2 controls.

Figure 2-3 and Figure 2-4 show the daily average soil moisture, precipitation, and irrigation events, while Figure 2-5 resumes the temperature data.

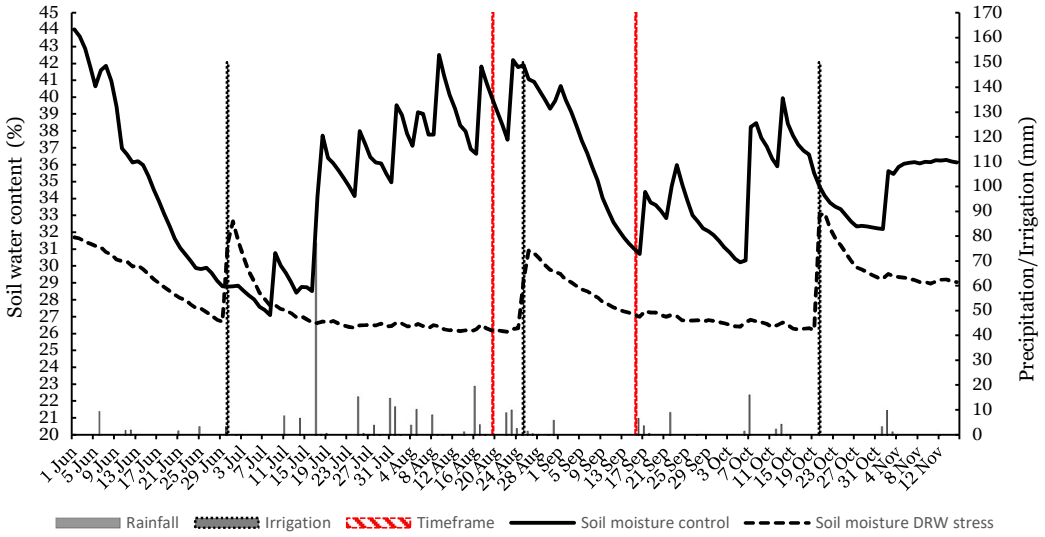

Figure 2-3. Evolution of daily averages for soil water content (%) (left axis) and water inputs (mm) (right axis) between June 1st and November 12th. The soil water content is differentiated by DRW (dashed line) and control (continued line) plots. The water inputs are differentiated by precipitation (black columns) and irrigation (dashed columns). The data analysed in the current thesis falls between the red lines.

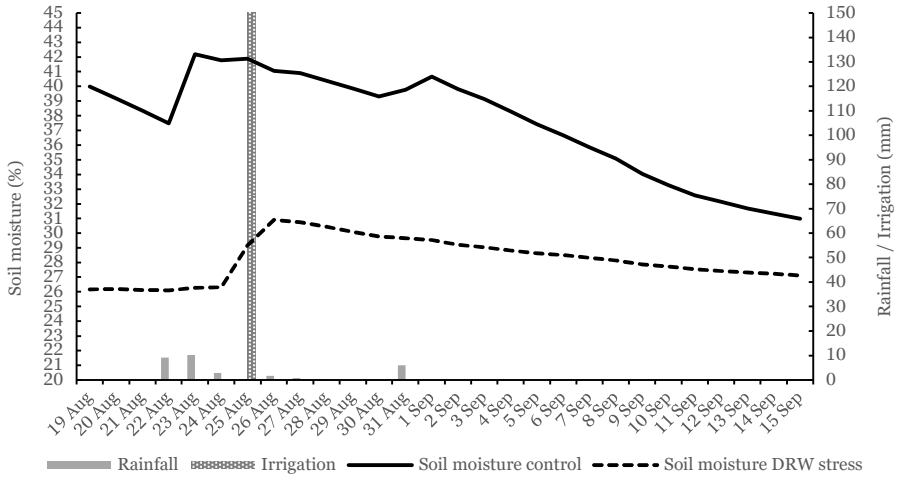

Figure 2-4. Evolution of daily averages for soil water content (%) (left axis) and water inputs (mm) (right axis) between August 19th and September 15th. The soil water content is differentiated by DRW (dashed line) and control (continued line) plots. The water inputs are differentiated by precipitation (solid columns) and irrigation (dotted columns).

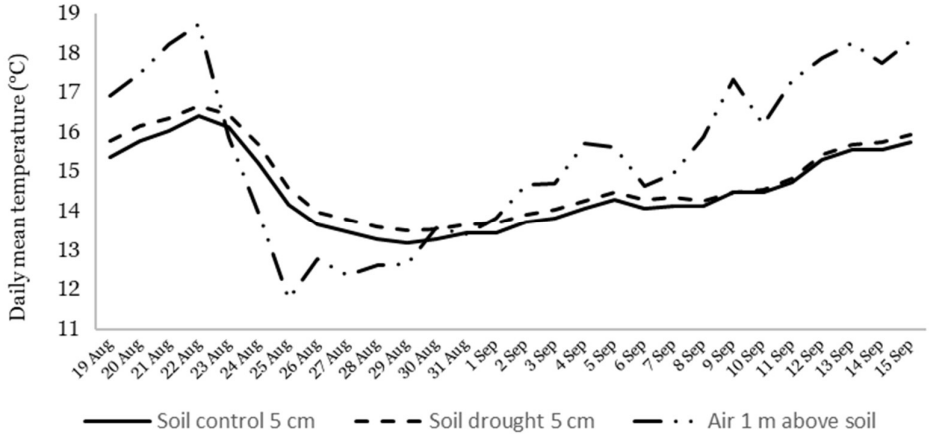

Figure 2-5. Evolution of daily averaged temperature between August 19th and September 15th, at 5 cm soil depth in control (solid line) and DRW stress (dashed line), and air temperature at 2 m above soil (dashed and pointed line). "drought" is referring to "DRW stress".

2.8. Data handling and statistical analysis

2.8.1. Software

For creating data frames, tables and figures, Microsoft Excel and RStudio were used (R Core Team, 2021; RStudio Team, 2021), but only the latter was used for the statistical analysis. Contour plots were performed with Surfer® (Golden Software, LLC).

2.8.2. Transformations

The simplest transformations were pooling and averaging the data to obtain daily means. This was the case for data with time resolution lower than intraday level, like CO_2 fluxes, soil moisture and temperature, air temperature, and precipitation. Since the soil sensors were installed 2 at sheltered and 2 at non-sheltered plots, it was necessary to pool this data into DRW stress and control treatments for posterior correlation and linear regression analysis with CO_2 fluxes.

However, some data was also log-transformed ($\log_{10}$) to achieve normality and reduce the effect of outliers, and this was the case for CO_2 efflux, and for many ancillary physicochemical soil parameters, before mean comparisons, correlation, or regression analysis.

2.8.3. Statistical tests

For multiple mean comparisons, i. e. when the 4 combination treatments (C, C+N, S, S+N) were compared, the first option was ANOVA, followed by Tukey's post hoc analysis. However, if the normality assumption could not be fulfilled, the Kruskal-Wallis's test was used, followed by Wilcoxon's sum rank test (with Bonferroni correction) as post-hoc analysis.

2.8.4. Validation

The validation approach of models was based on Zuur et al. (2007), and heteroscedasticity was tested by plotting the models' residuals against fitted values. A QQ-plot of the residuals was used for normality and residuals against every explanatory variable for independence.

3. Results

3.1. Spatial variability

The boxplots shown in Figure 3-1 were constructed combining flux data of two days (August 24th and 31st). The resultant pattern of CO_2 efflux across the plots is typical for the period analysed and gives an idea of the spatial variability of the setup. A Kruskal-Wallis's test was performed to explore differences by treatment using the two days fluxes, and although it was significant (P<0.05), Wilcoxon's sum rank test with Bonferroni's correction gave no difference between treatments. The mean and SD value for the 2 days was 228.0 ± 155.9 mg CO_2-C m^{-2} h^{-1}. If several days around the two dates are averaged, e. g. the sampling date and the 4 previous days, from August 20th to 24th (before rewetting) and from August 27th to 31st (after rewetting), the average flux and SD now is 229.7 ± 152.4 mg CO_2-C m^{-2} h^{-1}, almost the same result.

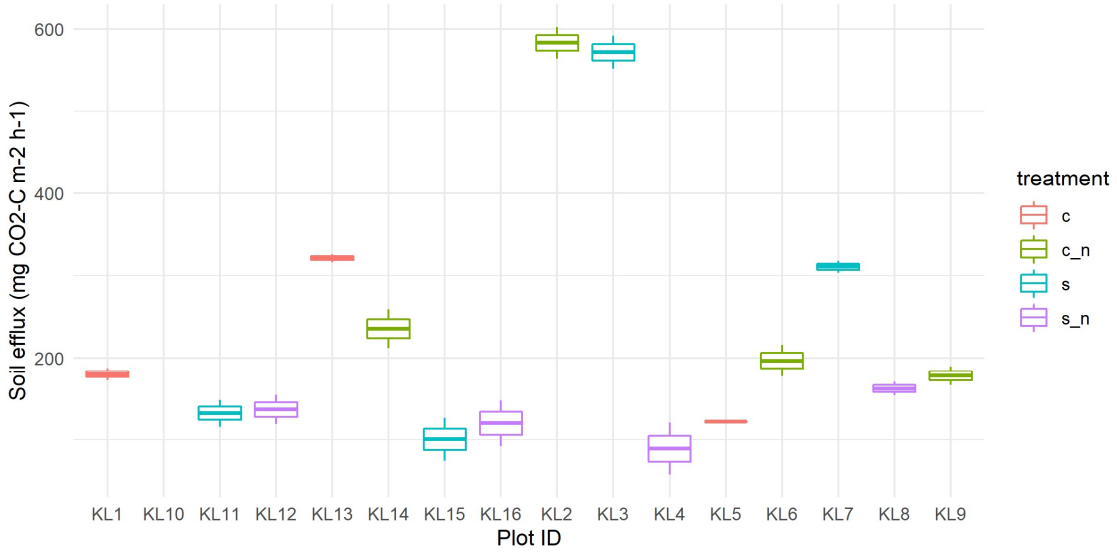

Figure 3-1. Boxplots of daily average soil efflux (CO_2-C m^{-2} h^{-1}) from each plot and coloured by the 4 treatments combination. Boxplots contain only data from August 24th and 31st.

For further assessing the contribution of the spatial variability in the soil CO_2 efflux, the ancillary soil data were grouped and compared by sampling date, before (August 24th) and after (August 31st), and by treatments (either by pp exclusion*N addition or only by pp exclusion). The significant results showed that the total N at 20 cm was higher (P<0.05) and the C:N ratio at 20 cm lower (P<0.05) for the DRW stress compared with control. Also, the lower C:N ratio at 20 cm value was for the "S" treatment. Also, the microbial biomass N was lower (P<0.05) for the DRW stress plots, but only on the first sampling date. The contrary happened with ammonium, being higher for the DRW plots but only at the second sampling date (P<0.05). The comparisons between the 4 treatments combined (C, C+N, S, and S+N) resulted in all the ANOVA and Kruskal-Wallis tests not being significant. The summarized data and p values are shown in Table 0-1(Appendix A).

On the other hand, the soil efflux data was correlated, and linear regressions were fitted with the soil parameters without any differentiation by date or treatment and the results are showed in Table 2-1 and Table 3-1. Significant Spearman's correlations were found for MBC at 10 cm (rho = 0.55; $P<0.01$) and at 20 cm depth (rho = 0.4; $P<0.05$), for MBN at 10 cm (rho = 0.5; $P<0.01$) and at 20 cm (rho = 0.43; $P<0.05$), and for DOC at 10 cm (rho = 0.39; $P<0.05$). Furthermore, the significant linear regressions were fitted for Total C at 20 cm ($R^2 = 0.14$; $P<0.05$; after log transforming), for MBC at 10 cm ($R^2 = 0.16$; $P<0.05$), for MBN at 10 cm ($R^2 = 0.16$; $P<0.05$), and for DOC at 10 cm ($R^2 = 0.14$; $P<0.05$). Lastly, a multiple linear regression which included the 4 variables of the simple linear regressions as explanatory variables, was almost significant ($R^2 = 0.19$; $P<0.065$; not included in the table).

Table 3-1. Soil parameters mean and SD. Rho Spearman's correlation and R^2 linear regression were calculated, relating the variables with the log-transformed (log_{10}) CO_2 efflux. Significance: * = $P<0.05$; ** = $P<0.01$. Transformation of the explanatory variables is indicated. Abbreviations: dw = soil dry weight; SD = standard deviation.

Parameter	Unit	Mean	SD	rho	R^2	Transformation?
Sand (10 cm)	%	13.4	3.43	0.30		
Sand (20 cm)	%	11	1.9	0.14		
Silt (10 cm)	%	55.2	4.36	<0.01		
Silt (20 cm)	%	54.4	3	<0.01		
Clay (10 cm)	%	31.42	4	-0.24		
Clay (20 cm)	%	34.8	2.9	-0.11		
Total N (10cm)	w/w%	0.19	0.06	0.09		
Total N (20cm)	w/w%	0.13	0.05	0.18		
Total C (10cm)	w/w%	3.6	0.8	0.04		
Total C (20cm)	w/w%	2.4	0.8	0.09	0.14*	Log
C:N (10cm)	-	19.4	3.2	-0.27		
C:N (20cm)	-	20.1	3.5	0.10		
Microbial biomass C (10 cm)	C mg $(kg\ dw)^{-1}$	144.6	43.51	0.55**	0.16*	
Microbial biomass C (20 cm)	C mg $(kg\ dw)^{-1}$	144.6	69.2	0.4*		
Microbial biomass N (10 cm)	N mg $(kg\ dw)^{-1}$	19.2	6.2	0.5**	0.16*	
Microbial biomass N (20 cm)	N mg $(kg\ dw)^{-1}$	20.2	9.5	0.43*		
Dissolved organic C (10 cm)	C mg $(kg\ dw)^{-1}$	207.7	35.4	0.39*	0.14*	
Dissolved organic C (20 cm)	C mg $(kg\ dw)^{-1}$	186	39	0.30		
Dissolved organic N (10 cm)	N mg $(kg\ dw)^{-1}$	25.9	5.6	0.29		
Dissolved organic N (20 cm)	N mg $(kg\ dw)^{-1}$	22.8	4.5	0.41		
NO_3^- (10 cm)	µg NO_3^--N $(g\ dw)^{-1}$	2.6	2.2	0.20		
NO_3^- (20 cm)	µg NO_3^--N $(g\ dw)^{-1}$	1.45	0.8	0.20		
NH_4^+ (10 cm)	µg NH_4^+-N $(g\ dw)^{-1}$	7.3	2.9	-0.04		
NH_4^+ (20 cm)	µg NH_4^+-N $(g\ dw)^{-1}$	5.6	1.8	0.05		

3.2. Temporal variability

Figure 3-2 and Figure 3-1 show similar patterns, but the new one includes all the average daily CO_2 efflux observations for each chamber, which is expressed as more vertical dispersion of the points and boxplots. Also, the overall mean and SD values were 222.5 ± 139.7 mg CO_2-C m^{-2} h^{-1}, showing the same or lower level of variation than the spatial analysis and similar mean value. However, for this case, the Kruskal-Wallis's test resulted significant (P<0.0001) for all the periods analysed, and the Welch's test when comparing before and after rewetting means (P<0.01 or lower). Wilcoxon's rank sum test showed treatments C+N and S with the highest mean flux, C with intermediate values, and S+N with the lowest (Table 3-2) for the three periods analysed.

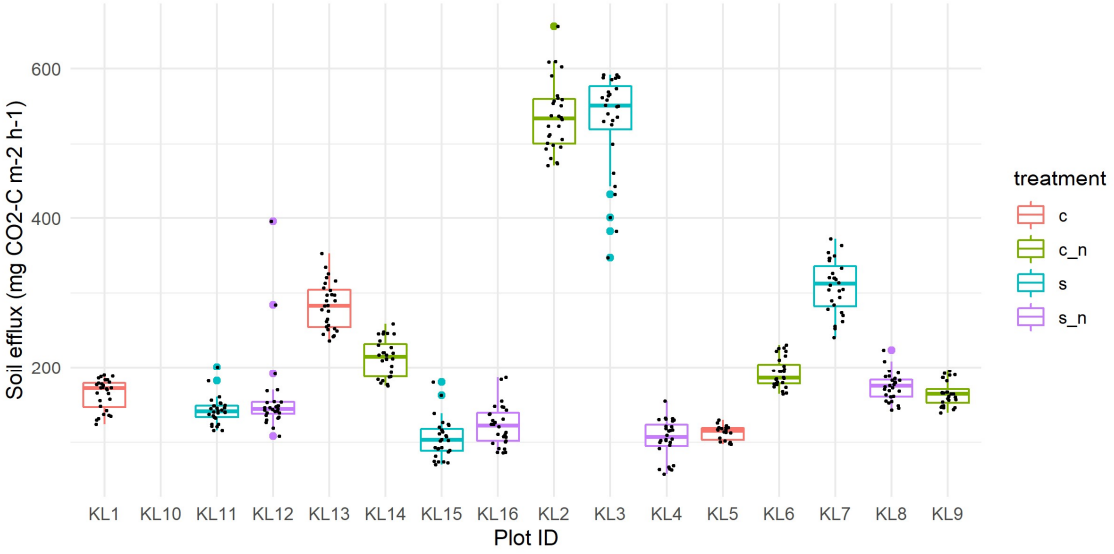

Figure 3-2. Boxplots of daily average soil efflux (CO_2-C m^{-2} h^{-1}) from each plot and coloured by the 4 treatments combination. The data for the full period (28 days) is included. The points in black are all the flux observations (28).

Table 3-2. Mean +- SE (min-max) of averaged CO_2 fluxes along days of the four treatments when including N addition levels. Three periods were considered, complete (28 days from August 19th to September 15th), before rewetting (6 days from August 19th to 24th), and after rewetting (22 days from August 25th to September 15th). The p-values inform the Kruskal-Wallis's test. The letters above the means indicate ranks from Wilcoxon's sum rank test with Bonferroni correction.

	mg CO_2-C m^{-2} h^{-1}				
	C	**C + N**	**S**	**S + N**	**p-value**
complete (28 d)	[b]200.14 +- 7.20 (154.95-287.41)	[a]276.69 +- 4.67 (241.99-329.3)	[a]271.25 +- 4.41 (232.29-306.08)	[c]140.37 +- 5.23 (103.22-226.10)	***<0.0001***
before rewett.(6 d)	[a]256.52 +- 8.82 (211.29-287.41)	[a]310.42 +- 5.62 (289.06-329.3)	[a]263.37 +- 7.84 (244.33-306.08)	[b]127.98 +- 16.7 (103.22-226.10)	***<0.0001***
after rewett. (22 d)	[b]181.34 +- 3.86 (154.95-206.72)	[a]265.44 +- 3.28 (241.99-287.3)	[a]273.87 +- 5.24 (232.29-299.92)	[b]144.50 +- 4.24 (118.30-211.62)	**<0.0001**
before vs. after-*p*-value	***<0.0001***	***<0.0001***	***0.008***	***<0.0001***	

However, a temporal series of the fluxes can help to better distinguish the temporal variation of the present dataset. Figure 3-3 shows the evolution of CO_2 efflux across the 4 treatments, which coincides with the data described in Table 3-2 in the emission ranking of the treatments. Furthermore, it shows high intraday variability (spatial probably), and a strong reaction to the irrigation, mainly on the first day (August 25th) and by the S+N treatment, while the S treatment shows a softer reaction.

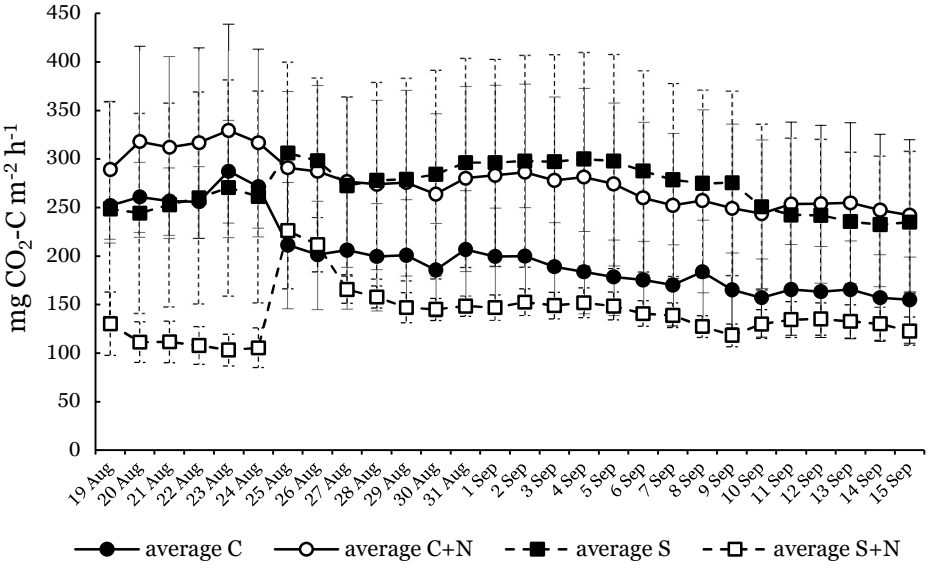

Figure 3-3. Time series of daily averaged soil CO_2 emission [mg CO_2-C m^{-2} h^{-1}], per treatment and including nitrogen addition levels, for the 28 days between August 19th and September 15th. Error bars indicate SE.

Similarly, Figure 3-4 also shows the evolution of soil CO_2 efflux in the entire period. However, the data is pooled by precipitation exclusion treatment and averaged, and the new feature here is the different behaviour of the DRW stress plots before and after the rewetting. Also, the average soil water content, natural precipitation, and the amount irrigated are shown. Both soil water content and the CO_2 efflux from the stressed soil react to the irrigation. However, the soil water content in the control plots was more sensitive to water inputs, which is also better and more detailed shown in Figure 2-3 and Figure 2-4. Lastly, the flux curves, mainly control, seem to be coupled with the soil water content.

The fluxes were, on average lower during the 28-d-period (P<0.01) and before the rewetting (P<0.01) for the stressed plots. Also, the control fluxes were higher before (P<0.05) the rewetting. Most importantly, there was no significant difference after the rewetting despite lower soil moisture at the stressed plots (Table 3-3).

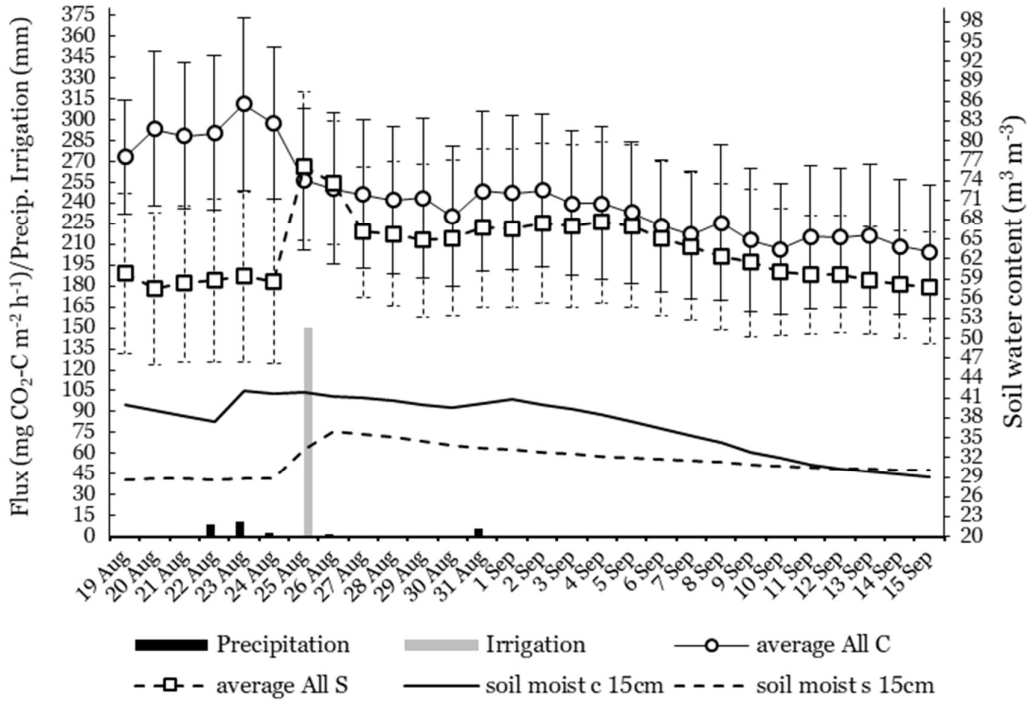

Figure 3-4. Time series of daily averaged soil CO_2 emission [mg CO_2-C m^{-2} h^{-1}] (left axis) and soil water content [m^3 m^{-3}] (right axis), and precipitation/irrigation [mm] (left axis) for the 28 days between August 19th and September 15th, and considering only the rainfall manipulation (pooled and averaged into Average All S and C). Error bars indicate SE.

Table 3-3. Mean +- SE (min-max) of averaged CO_2 fluxes [mg CO_2-C m^{-2} h^{-1}] along days of the two levels of the rainfall manipulation. Three periods were considered, complete (28 days from August 19th to September 15th), before rewetting (6 days from August 19th to 24th), and after rewetting (22 days from August 25th to September 15th). The p-values inform Welch's test results.

	mg CO_2-C m^{-2} h^{-1}		
	control	**DRW stress**	**p-value**
complete (28 d)	243.90 +-5.69 (204.7-311.3)	205.80 +- 4.33 (177.8-266.1)	***0.008***
before rewett. (6 d)	290.50 +- 5.08 (273.1-311.3)	183.46 +- 1.63 (177.8-189.1)	***0.002***
after rewett. (22 d)	245.60 +- 3.51 (204.7-256.9)	211.78 +- 4.75 (178.9-266.1)	*0.2*
before vs after *p*-value	***0.028***	0.065	

3.3. Meteorological data

The data related to soil water content and temperature, both differentiated only by precipitation exclusion treatment, and data on precipitation and air temperature were already shown in Figure 2-3, Figure 2-4, Figure 2-5, and Figure 3-4. The means of this data were also tested for

exploring differences. The soil temperature (at 5 cm depth) was similar between treatments but showed a decrease (P<0.0001) from the beginning to the end of the analysis period (Table 3-4).

Table 3-4. Mean +- SE (min-max) of the daily mean soil temperature at 5 cm depth [°C] for "control" and "drought" plots averaged and differentiated by period. Three periods were considered, complete (28 days from August 19th to September 15th), before rewetting (6 days from August 19th to 24th), and after rewetting (22 days from August 25th to September 15th). The p-values inform Student's t-test results.

	Soil temperature 5 cm (°C)		
	control	**DRW stress**	**p-value**
complete (28 d)	14.54 +- 0.19 (13.21-16.42)	14.78 +- 0.19 (13.52-16.66)	0.38
before rewett. (6 d)	15.53 +- 0.19 (15.21-16.42)	16.18 +- 0.16 (15.68-16.66)	0.18
after rewett. (22 d)	14.19 +- 0.17 (13.21-15.76)	14.40 +- 0.16 (13.52-15.96)	0.37
before vs afer p-value	***<0.0001***	***<0.0001***	

Figure 2-3 allocates the current thesis analysis period at a moment of maximum difference in soil water content between the treatments. It also shows the already mentioned higher sensitivity to reaction for the control plots. Figure 2-4 zooms in and allows us to see how an irrigation event of 150 mm had the same positive effect as the control plots showed for natural precipitation of ~20 mm, which will be discussed later. Lastly, Table 3-5 summarizes the results of the Student's t-tests, showing higher moisture contents (P<0.0001) for the control plots during all the periods analysed and was also higher before the rewetting (P<0.05). The DRW stress also shows an increase (P<0.0001), but it is being dissolved by the longer 22 days period chosen, so the increase is better seen in the mentioned figures.

Table 3-5. Mean +- SE (min-max) of daily mean soil water content at 15 cm depth [%] for "control" and "drought" plots averaged and differentiated by period. Three periods were considered, complete (28 days from August 19th to September 15th), before rewetting (6 days from August 19th to 24th), and after rewetting (22 days from August 25th to September 15th). The p-values inform Welch's t-test results.

	Soil moisture 15 cm (%)		
	control	**DRW stress**	**p-value**
complete (28 d)	37.54 +- 0.67 (30.98-42.18)	28.23 +- 0.28 (26.10-30.91)	***<0.0001***
before rewett. (6 d)	39.82 +- 0.76 (37.48-42.18)	28.07 +- 0.03 (26.10-26.31)	***<0.0001***
after rewett. (22 d)	36.92 +- 0.78 (30.98-41.88)	28.78 +- 0.25 (27.10-30.91)	***<0.0001***
before vs afer p-value	***0.017***	***<0.0001***	

3.4. Regression analysis

Table 3-6 shows the simple and multiple regression models that were significant and showed higher R^2 values. Daily averages of CO_2 fluxes strongly correlated with soil water content and

temperature, in that order in both "control" and "DRW stress" treatments. Furthermore, the multiple regression model relating the CO_2 efflux from control treatment with the soil moisture and temperature as first and second regressor variables showed an R^2-value of 0.95, with a positive correlation with soil moisture and temperature. Besides, another linear regression fitted for the DRW stress treatment resulted in soil moisture as a single regressor explaining 66% of the variability on the emission, with a slope value of 12.41. The same model was fitted for the control treatment, and the soil moisture explained 54% of the variation, with a slope of 6.2. On the other hand, soil temperature contrasted in behaviour inside treatments since it correlated positively in "control" but negatively in "DRW stress". Similar values (R^2 and slope) were obtained using another approach, with the automatic curve fitting function in Microsoft Excel (Figure 0-1 and Figure 0-2, Appendix A).

Table 3-6. Simple and multiple regression analysis between mean daily CO_2 fluxes against soil temperature and moisture. Pearson's R^2 was informed. Significance: * p<0.05, ** p<0.01, *** p<0.001.

	Rainfall manipulation treatment							
Treatment	**Control**		**Control**		**DRW**		**DRW**	
Dependent variable *yt*	mg CO_2-C m^{-2} h^{-1}							
Intercept β_0	11.1		-373.1	***	-144.52	**	450.16	***
Regression coefficients:								
(Soil water content) β_i	6.2	***	8.3	***	12.41	***	--	
(Soil temperature) β_i	--		21	***	--		-16.53	***
Total R^2:	**0.54**		**0.95**		**0.66**		**0.52**	
n	28		28		28		28	

3.5. Contour plots

Contour plots are another graphical alternative to represent the relation between variables, like emission, soil temperature, and soil moisture. Figure 3-5 and Figure 3-6 need to be analysed separately, but in general, the higher the soil temperature and water content, the darker the colour, the higher the soil CO_2 efflux (darker colour). Figure 3-7, which mixes all the values together, has two clouds at mid-low temperature and moisture values, probably corresponding to the pulse after rewetting in the DRW stress treatment.

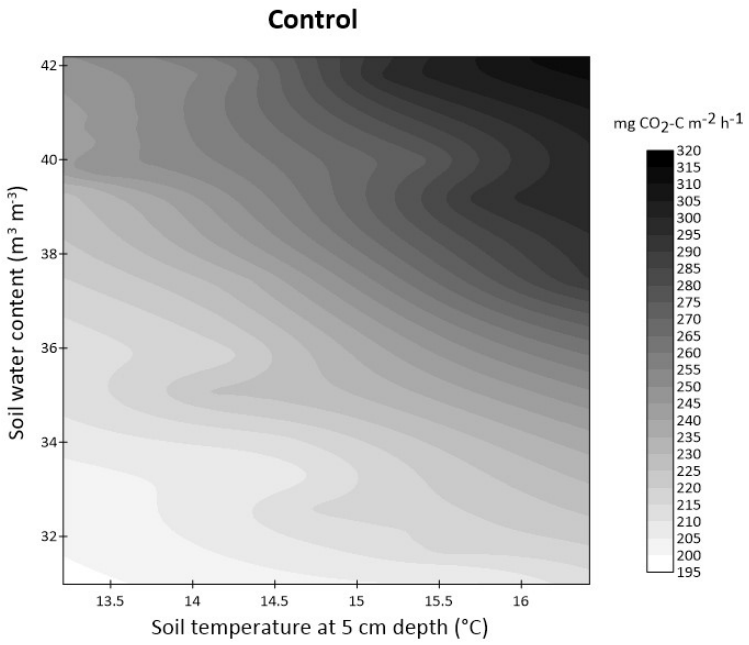

Figure 3-5. Contour map of soil fluxes driven by soil temperature and soil water content in the control treatment. Elaborated with Surfer® (Golden Software, LLC).

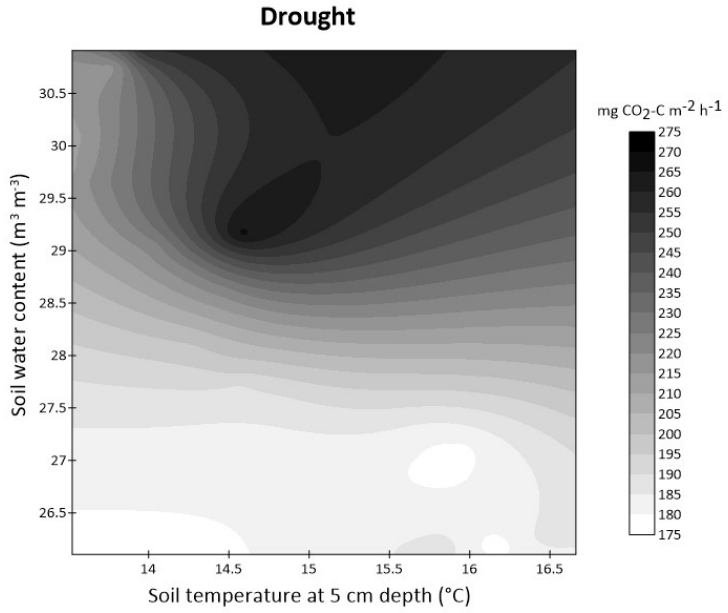

Figure 3-6. Contour map of soil fluxes driven by soil temperature and soil water content in drought treatment. Elaborated with Surfer® (Golden Software, LLC). “Drought” stands for “DRW stress” treatment.

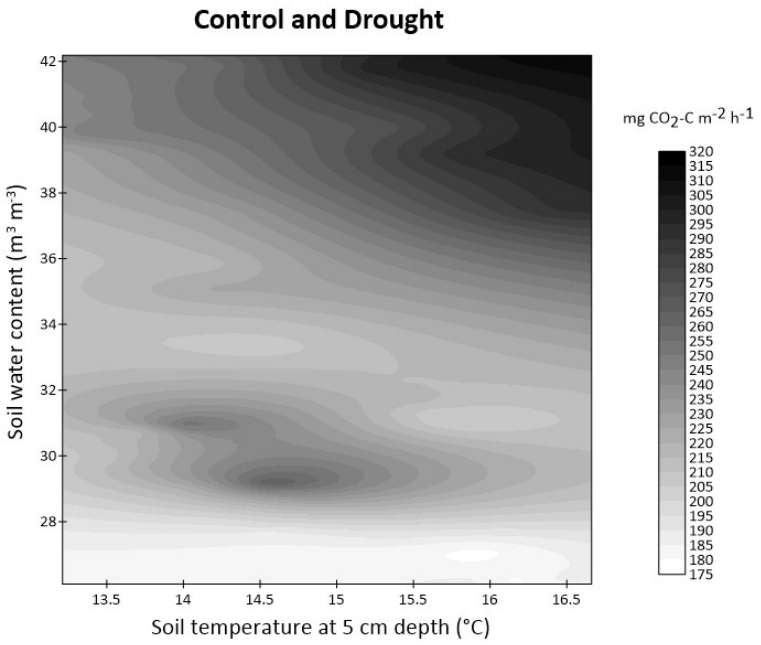

Figure 3-7. Contour map of soil fluxes driven by soil temperature and soil water content in all observations, control and drought treatments combined. Elaborated with Surfer® (Golden Software, LLC). “Drought” stands for “DRW stress” treatment.

4. Discussion

The first hypothesis assumed that the rewet of severely dry soil is expected to reactivate the microbial activity, and so soil CO_2 efflux and MBC would raise after irrigation. The results presented for the temporal variability (section 3.2), including the time series presented in Figure 3-3 and Figure 3-4, which show a strong increase in S and DRW emission on date August 25th, and the significant statistical tests in Table 3-2, support an increased CO_2 efflux after rewetting up to the level of the control. Furthermore, although MBC did not significantly increase after rewetting, it was found a significant correlation between soil CO_2 efflux and MBC at 10 (rho = 0.55; P<0.01) and 20 (rho = 0.4; P<0.05) cm depth and also a linear regression model was fitted (R^2=0.16; P<0.05; Table 3-1). Likewise, a positive correlation (R^2= 0.52) between soil CO_2 and MBC was also found by Lee & Jose (2003) in a temperate ecosystem. Also, Navarro-García et al. (2011), in a manipulative experiment to assess the effect of aggregation in controlling the microbial response during DRW cycles, found that aggregate destruction, which can also be promoted by DRW cycles, can release occluded C, which can subsequently enhance both R_s and microbial biomass. In the same line, Zhao et al. (2010) also found that increased frequency of DRW cycles, and fertilization events, enhanced not only MBC but also DOC. However, in an incubation study by Sawada et al. (2017), although they found a pulse of R_s due after the DRW cycle, they also described a reduction of MBC whose magnitude relied on soil properties and the history of DRW cycles, where the microbial community in soils with more frequent DRW are better adapted, and so the MBC can be maintained (also demonstrated by Leizaga et al., 2021). These results agree with the current study, where there was no detectable change in the MBC pool. Furthermore, it would be important to monitor what happens in the posterior DRW cycles at Klausen-Leopoldsdorf, to explore if there is really a moderation effect with the increasing history of DRW stress.

Many of the works cited in the previous paragraph did find a pulse after rewetting, and this is the topic of the next hypothesis. The Birch effect can be identified when there is a decoupling of the increasing rate in soil moisture and the R_s pulse, meaning that there is an exacerbated positive response upon an amount of water added over severely dry soil, which does not cause the same R_s pulse in continually moist soil. According to the results also deployed in section 3.2 ("Temporal variability"), there might be some evidence supporting there was a Birch effect pulse type in Rs in the DRW stress treatment. One hint is the sharp increase in S+N treatment shown in Figure 3-3. Also, Table 3-2 shows that although both C and C+N emissions declined in the second period starting on August 25th, at the same time, both S and S+N increased. Likewise, Table 3-3 showed no significant difference between the two pooled treatments (control and DRW stress), and DRW emission might have even surpassed the control level (Figure 3-4). However, the soil in DRW plots have much less water content (Figure 2-4 and Figure 3-4), which is not justified by differences in texture (Table 0-1, Appendix A) and probably neither in structure. Hence, this supports the hypothesis that there was a decoupling between R_s and soil moisture. Also, a plot of the ratio DRW:Control efflux against the ratio of soil moisture (soil moisture in DRW over soil moisture in Control) shows an abrupt jump around a value of 0.7 of the "ratio moisture s/c", which can support the decoupling (**see Figure 0-3, Appendix A**). Furthermore, a moderate increase in water availability accompanying a

moderate Birch effect is supported by previous studies. For example, Barnard et al. (2020) proposed the magnitude of the rewetting upshock controls the rate of availability of labile C that feeds the pulse and that upon a certain threshold, occlude organic matter becomes accessible, which was probably not the case at Klausen-Leopoldsdorf in the current DRW cycle, but there was a detection of increased NH_4^+ upon rewetting ($P<0.05$; Table 0-1), possibly suggesting increased mineralization of organic N, and microbial death can be a source of released C and N labile forms after rewetting (Blazewicz et al., 2014).

A decoupling of the R_s from either the soil moisture and/or the soil temperature is not the rule, but rather the exception in the soil. The third hypothesis assumes these two variables are strong drivers of the R_s. However, the soil moisture can be limiting either by scarcity or abundance, becoming a stronger driver than temperature (Borken et al., 1999; Epron et al., 2004; Yuste et al., 2005), and since there was water limitation (simulated by rainfall exclusion manipulation), it can be expected a strong positive correlation between R_s and soil moisture. The regression models in Table 3-6 support the idea that both variables were important drivers, even though maybe it was not expected from the temperature. However, soil moisture was stronger as a predictor and had a positive relation. Similar results have been found by Kitzler et al. (2006) at the same site. Notwithstanding, what was maybe not expected was the high variability not explained by moisture and temperature that can be attributed to spatial variability among plots and will be discussed in the next hypothesis. What also remains elusive is the fate of the irrigation water. The soil water content in the control plots was much more sensitive to inputs since it can be seen in its pulses to natural precipitation events, e. g. of a magnitude ~20 mm in two consecutive days (August 22nd and 23rd; Figure 2-4). This event generated an absolute increase of ~5% in the soil water content, while by the irrigation event of 150 mm, the DRW plots increased ~5%. This would be interesting to explore further. One possible explanation would be that the rate of precipitation surpasses the capacity of the soil to retain the water, which loses it by deep percolation or superficial sub-superficial runoff. In line with this, drought can promote hydrophobicity (Goulden et al., 1996), which would enhance superficial runoff. However, a superficial runoff was not detected in the field.

There were several hints pointing at the existence of a high variability among plots in the current setup. We hypothesized that since forest soils show high variability of soil biochemical and physical parameters, CO_2 efflux would also show high spatial variability, and it would be possible to find correlations with any of the biochemical and physical soil parameters monitored. The importance of spatial variability among plots in the current study can be depicted by comparing Figure 3-1 vs Figure 3-2. While the first one only includes spatial variability because it is reduced to only two days, the second one includes the 28 measurements of the entire period analysed. Surprisingly, they are very similar, meaning that the added temporal variability might not be so important. Also, the time series plots Figure 3-3 and Figure 3-4 also denote a huge variability at every daily average, represented by the error bars (error standard). The explanatory power over R_s of the spatial variability has been studied not only in forests soils but also in general when studying trace gas flux emissions (Bahn et al., 2008; Curiel Yuste et al., 2004; Epron et al., 2004b; Kang et al., 2003; Law et al., 2001; Søe & Buchmann, 2005; Vincent et al., 2006). For example, Søe & Buchmann (2005) working on a beech forest in Germany, developed heat maps of R_s and correlated them with several soil and vegetation parameters. This allows them to identify “hotspots” of emission. In the current set-

up, we might be able to also find them. For example, the high emission of plots 2 and 3 might correspond with hotspots. Here it might be important to check if autotrophic (plant roots and rhizospheric) respiration is inflating the emission. With the purpose of disentangling the spatial patterns of R_s in the current setup, the correlations and regressions shown in Table 3-1 were performed. The exploration resulted in the identification of a few parameters with some potential to explain R_s spatial heterogeneity. Those were Total carbon at 10 cm (log-transformed), MBC at 10 cm, MBN at 10 cm, and DOC at 10 cm, which along with other variables (e.g. pH, Bulk density, Litter layer depth), were also found to explain R_s in others works (Bahn et al., 2008; Curiel Yuste et al., 2004; Epron et al., 2004b; Kang et al., 2003; Law et al., 2001; Søe & Buchmann, 2005; Vincent et al., 2006). Assessing spatial variability would be essential to future model attempts of R_s.

Finally, another expectation was that enrichment of forest soils with N_r would increase the concentration of mineral forms of N, either NO_3^- or NH_4^+, reduce microbial activity (MBC), and suppress soil CO_2 efflux. Among the results, the only significant difference found when comparing the N addition treatment was in C:N ratio at 20 cm. However, even this difference might not have been caused by the N treatment since it gave the opposite results, showing lower values (higher N content) for the untreated soil. Furthermore, there was a not expected pattern in the R_s (Table 3-2), while R_s might have been enhanced by the N addition in the control plots, there was a suppression effect in the DRW stress treatment. The latter effect might be explained by the combination of the expected depression effect that N_r has been described to have in the R_s (Dirnböck et al., 2017; Janssens et al., 2010; Pregitzer et al., 2008; Zhou et al., 2014; Zhong et al., 2016), and the suppression by DRW stress which can also hamper the R_s. However, further exploration might shed light on whether this apparent enhancing effect of the N addition on the control plots is reproducible or if it is a product of spatial variability.

5. Conclusions

The present study offers a reliable set of measurements of soil respiration of a mature temperate forest and an effort to disentangle the contribution of soil parameters on the temporal and spatial variability under a simulated scenario of increased dry-rewetting stress and atmospheric N_r deposition.

This thesis found evidence suggesting the occurrence of a moderated Birch effect and a rapid recovery of the soil respiration upon rewetting. Also, this response would be leaded not only by soil moisture content but by other soil parameters, which enhances the spatial variability of the soil respiration.

Although soil moisture and temperature were found to be the most important drivers of soil respiration, a vast spatial variability has been described, and the current study gives preliminary clues over which soil parameters might be driving that.

Furthermore, this thesis tried to distinguish between the Birch effect and the soil moisture, which usually overlap.

Finally, the analysis of the effect of atmospheric N_r deposition throws a new pattern which must be confirmed with further exploration.

References

Almagro, M., J. López, J. I. Querejeta, and M. Martínez-Mena. 2009. "Temperature Dependence of Soil CO_2 Efflux Is Strongly Modulated by Seasonal Patterns of Moisture Availability in a Mediterranean Ecosystem." *Soil Biology and Biochemistry* 41 (3): 594–605. https://doi.org/10.1016/j.soilbio.2008.12.021.

Anav, Alessandro, Pierre Friedlingstein, Christian Beer, Philippe Ciais, Anna Harper, Chris Jones, Guillermo Murray-Tortarolo, et al. 2015. "Reviews of Geophysics Primary Production : A Review." *Reviews of Geophysics*, 1–34. https://doi.org/10.1002/2015RG000483.Received.

Bahn, M., M. Reichstein, E. A. Davidson, J. Grünzweig, M. Jung, M. S. Carbone, D. Epron, et al. 2010. "Soil Respiration at Mean Annual Temperature Predicts Annual Total across Vegetation Types and Biomes." *Biogeosciences* 7 (7): 2147–57. https://doi.org/10.5194/bg-7-2147-2010.

Barnard, Romain L., Steven J. Blazewicz, and Mary K. Firestone. 2020. "Rewetting of Soil: Revisiting the Origin of Soil CO_2 Emissions." *Soil Biology and Biochemistry* 147 (April): 107819. https://doi.org/10.1016/j.soilbio.2020.107819.

Barnard, Romain L., Catherine A. Osborne, and Mary K. Firestone. 2015. "Changing Precipitation Pattern Alters Soil Microbial Community Response to Wet-up under a Mediterranean-Type Climate." *ISME Journal* 9: 946–57. https://doi.org/10.1038/ismej.2014.192.

Bimüller, Carolin, Michael Dannenmann, Javier Tejedor, Margit von Lützow, Franz Buegger, Rudolf Meier, Stephan Haug, Reiner Schroll, and Ingrid Kögel-Knabner. 2014. "Prolonged Summer Droughts Retard Soil N Processing and Stabilization in Organo-Mineral Fractions." *Soil Biology and Biochemistry* 68: 241–51. https://doi.org/10.1016/j.soilbio.2013.10.003.

Birch, H. F. 1958. "The Effect of Soil Drying on Humus Decomposition and Nitrogen Availability." *Plant and Soil* 10 (1): 9–31. https://doi.org/10.1007/BF01343734.

Blankinship, Joseph C., and Joshua P. Schimel. 2018. "Biotic versus Abiotic Controls on Bioavailable Soil Organic Carbon." *Soil Systems* 2 (1): 1–13. https://doi.org/10.3390/soilsystems2010010.

Bond-Lamberty, Ben, and Allison Thomson. 2010. "Temperature-Associated Increases in the Global Soil Respiration Record." *Nature* 464 (7288): 579–82. https://doi.org/10.1038/nature08930.

Borken, Werner, and Egbert Matzner. 2009. "Reappraisal of Drying and Wetting Effects on C and N Mineralization and Fluxes in Soils." *Global Change Biology* 15 (4): 808–24. https://doi.org/10.1111/j.1365-2486.2008.01681.x.

Borken, Werner, Yi Jun Xu, Eric A. Davidson, and Friedrich Beese. 2002. "Site and Temporal Variation of Soil Respiration in European Beech, Norway Spruce, and Scots

Pine Forests." *Global Change Biology* 8 (12): 1205–16. https://doi.org/10.1046/j.1365-2486.2002.00547.x.

Butterbach-Bahl, Klaus, Ralf Kiese, and Chunyan Liu. 2011. *Measurements of Biosphere Atmosphere Exchange of CH 4 in Terrestrial Ecosystems*. *Methods in Enzymology*. 1st ed. Vol. 495. Elsevier Inc. https://doi.org/10.1016/B978-0-12-386905-0.00018-8.

Canadell, J.G., P.M.S. Monteiro, M.H. Costa, L. Cotrim da Cunha, P.M. Cox, A.V. Eliseev, S. Henson, M. Ishii, S. Jaccard, C. Koven, A. Lohila, P.K. Patra, S. Piao, J. Rogelj, S. Syampungani, S. Zaehle, and K. Zickfeld, 2021: Global Carbon and other Biogeochemical Cycles and Feedbacks. In Climate Change 2021: The Physical Science Basis. Contribution of Working Group I to the Sixth Assessment Report of the Intergovernmental Panel on Climate Change [Masson-Delmotte, V., P. Zhai, A. Pirani, S.L. Connors, C. Péan, S. Berger, N. Caud, Y. Chen, L. Goldfarb, M.I. Gomis, M. Huang, K. Leitzell, E. Lonnoy, J.B.R. Matthews, T.K. Maycock, T. Waterfield, O. Yelekçi, R. Yu, and B. Zhou (eds.)]. Cambridge University Press, Cambridge, United Kingdom and New York, NY, USA, pp. 673–816, doi:10.1017/9781009157896.007.

Conant, Richard T., Michael G. Ryan, Göran I. Ågren, Hannah E. Birge, Eric A. Davidson, Peter E. Eliasson, Sarah E. Evans, et al. 2011. "Temperature and Soil Organic Matter Decomposition Rates - Synthesis of Current Knowledge and a Way Forward." *Global Change Biology* 17 (11): 3392–3404. https://doi.org/10.1111/j.1365-2486.2011.02496.x.

Cooper, Mendel. 2010. "Advanced Bash-Scripting Guide An in-Depth Exploration of the Art of Shell Scripting Table of Contents." *Okt 2005 Abrufbar Uber Httpwww Tldp OrgLDPabsabsguide Pdf Zugriff 1112 2005* 2274 (November 2008): 2267–74. https://doi.org/10.1002/hyp.

Cosby, B. J., G. M. Hornberger, R. B. Clapp, and T. R. Ginn. 1984. "A Statistical Exploration of the Relationships of Soil Moisture Characteristics to the Physical Properties of Soils." *Water Resources Research* 20 (6): 682–90. https://doi.org/10.1029/WR020i006p00682.

Cosentino, Diego, Claire Chenu, and Yves Le Bissonnais. 2006. "Aggregate Stability and Microbial Community Dynamics under Drying-Wetting Cycles in a Silt Loam Soil." *Soil Biology and Biochemistry* 38 (8): 2053–62. https://doi.org/10.1016/j.soilbio.2005.12.022.

Curiel Yuste, J., D. D. Baldocchi, A. Gershenson, A. Goldstein, L. Misson, and S. Wong. 2007. "Microbial Soil Respiration and Its Dependency on Carbon Inputs, Soil Temperature and Moisture." *Global Change Biology* 13 (9): 2018–35. https://doi.org/10.1111/j.1365-2486.2007.01415.x.

Curiel Yuste, J., I. A. Janssens, A. Carrara, L. Meiresonne, and R. Ceulemans. 2003. "Interactive Effects of Temperature and Precipitation on Soil Respiration in a Temperate Maritime Pine Forest." *Tree Physiology* 23 (18): 1263–70. https://doi.org/10.1093/treephys/23.18.1263.

Curiel Yuste, J., I. A. Janssens, and R. Ceulemans. 2005. "Calibration and Validation of an Empirical Approach to Model Soil CO_2 Efflux in a Deciduous Forest." *Biogeochemistry* 73 (1): 209–30. https://doi.org/10.1007/s10533-004-7201-1.

Davidson, Eric A., and Ivan A. Janssens. 2006. “Temperature Sensitivity of Soil Carbon Decomposition and Feedbacks to Climate Change.” *Nature* 440 (7081): 165–73. https://doi.org/10.1038/nature04514.

Davidson, Eric A., Ivan A. Janssens, and Yiqi Lou. 2006. “On the Variability of Respiration in Terrestrial Ecosystems: Moving beyond Q10.” *Global Change Biology* 12 (2): 154–64. https://doi.org/10.1111/j.1365-2486.2005.01065.x.

Dilustro, John J., Beverly Collins, Lisa Duncan, and Chris Crawford. 2005. “Moisture and Soil Texture Effects on Soil CO_2 Efflux Components in Southeastern Mixed Pine Forests.” *Forest Ecology and Management* 204 (1): 87–97. https://doi.org/10.1016/j.foreco.2004.09.001.

Dirnböck, T., C. Foldal, I. Djukic, J. Kobler, E. Haas, R. Kiese, and B. Kitzler. 2017. “Historic Nitrogen Deposition Determines Future Climate Change Effects on Nitrogen Retention in Temperate Forests.” *Climatic Change* 144 (2): 221–35. https://doi.org/10.1007/s10584-017-2024-y.

Engardt, Magnuz, David Simpson, Margit Schwikowski, and Lennart Granat. 2017. “Deposition of Sulphur and Nitrogen in Europe 1900–2050. Model Calculations and Comparison to Historical Observations.” *Tellus, Series B: Chemical and Physical Meteorology* 69 (1): 1–20. https://doi.org/10.1080/16000889.2017.1328945.

Epron, Daniel, Lætitia Farque, Éric Lucot, and Pierre Marie Badot. 1999. “Soil CO2 Efflux in a Beech Forest: Dependence on Soil Temperature and Soil Water Content.” *Annals of Forest Science* 56 (3): 221–26. https://doi.org/10.1051/forest:19990304.

Epron, Daniel, Yann Nouvellon, Olivier Roupsard, Welcome Mouvondy, André Mabiala, Laurent Saint-André, Richard Joffre, et al. 2004. “Spatial and Temporal Variations of Soil Respiration in a Eucalyptus Plantation in Congo.” *Forest Ecology and Management* 202 (1–3): 149–60. https://doi.org/10.1016/j.foreco.2004.07.019.

Evans, Sarah, Ulf Dieckmann, Oskar Franklin, and Christina Kaiser. 2016. “Synergistic Effects of Diffusion and Microbial Physiology Reproduce the Birch Effect in a Micro-Scale Model.” *Soil Biology and Biochemistry* 93: 28–37. https://doi.org/10.1016/j.soilbio.2015.10.020.

Fernández-Alonso, María José, Jorge Curiel Yuste, Barbara Kitzler, Carlos Ortiz, and Agustín Rubio. 2018. “Changes in Litter Chemistry Associated with Global Change-Driven Forest Succession Resulted in Time-Decoupled Responses of Soil Carbon and Nitrogen Cycles.” *Soil Biology and Biochemistry* 120 (October 2017): 200–211. https://doi.org/10.1016/j.soilbio.2018.02.013.

Fernández-Alonso, María José, Eugenio Díaz-Pinés, Carlos Ortiz, and Agustín Rubio. 2018. “Disentangling the Effects of Tree Species and Microclimate on Heterotrophic and Autotrophic Soil Respiration in a Mediterranean Ecotone Forest.” *Forest Ecology and Management* 430 (August): 533–44. https://doi.org/10.1016/j.foreco.2018.08.046.

Fernández-Alonso, María José, Eugenio Díaz-Pinés, and Agustín Rubio. 2021. "Drivers of Soil Respiration in Response to Nitrogen Addition in a Mediterranean Mountain Forest." *Biogeochemistry* 155 (3): 305–21. https://doi.org/10.1007/s10533-021-00827-2.

Fierer, Noah, and Joshua P. Schimel. 2002. "Effects of Drying-Rewetting Frequency on Soil Carbon and Nitrogen Transformations." *Soil Biology and Biochemistry* 34 (6): 777–87. https://doi.org/10.1016/S0038-0717(02)00007-X.

Fierer, Noah, and Joshua P. Schimel. 2003. "A Proposed Mechanism for the Pulse in Carbon Dioxide Production Commonly Observed Following the Rapid Rewetting of a Dry Soil." *Soil Science Society of America Journal* 67 (3): 798. https://doi.org/10.2136/sssaj2003.0798.

Freedman, Bill. 2014. "Global Environmental Change." *Global Environmental Change* 38: 1–973. https://doi.org/10.1007/978-94-007-5784-4.

Friedlingstein, Pierre, Matthew W Jones, Michael O Sullivan, Robbie M Andrew, Dorothee C E Bakker, Judith Hauck, Corinne Le Quéré, Glen P Peters, and Wouter Peters. 2022. "Global Carbon Budget 2021," 1917–2005.

Göransson, Hans, Douglas L. Godbold, David L. Jones, and Johannes Rousk. 2013. "Bacterial Growth and Respiration Responses upon Rewetting Dry Forest Soils: Impact of Drought-Legacy." *Soil Biology and Biochemistry* 57: 477–86. https://doi.org/10.1016/j.soilbio.2012.08.031.

Goulden, Michael L., J. William Munger, Song Miao Fan, Bruce C. Daube, and Steven C. Wofsy. 1996. "Exchange of Carbon Dioxide by a Deciduous Forest: Response to Interannual Climate Variability." *Science* 271 (5255): 1576–78. https://doi.org/10.1126/science.271.5255.1576.

Goulden, Michael L., J. William Munger, Song Miao Fan, Bruce C. Daube, and Steven C. Wofsy. 1996. "Measurements of Carbon Sequestration by Long-Term Eddy Covariance: Methods and a Critical Evaluation of Accuracy." *Global Change Biology* 2 (3): 169–82. https://doi.org/10.1111/j.1365-2486.1996.tb00070.x.

Granier, A. et al. (2003). Deciduous Forests: Carbon and Water Fluxes, Balances and Ecophysiological Determinants. In: Valentini, R. (eds) Fluxes of Carbon, Water and Energy of European Forests. Ecological Studies, vol 163. Springer, Berlin, Heidelberg. https://doi.org/10.1007/978-3-662-05171-9_4

Green, Julia K., Sonia I. Seneviratne, Alexis M. Berg, Kirsten L. Findell, Stefan Hagemann, David M. Lawrence, and Pierre Gentine. 2019. "Large Influence of Soil Moisture on Long-Term Terrestrial Carbon Uptake." *Nature* 565 (7740): 476–79. https://doi.org/10.1038/s41586-018-0848-x.

Hartley, Iain P., Tim C. Hill, Sarah E. Chadburn, and Gustaf Hugelius. 2021. "Temperature Effects on Carbon Storage Are Controlled by Soil Stabilisation Capacities." *Nature Communications* 12 (1): 1–7. https://doi.org/10.1038/s41467-021-27101-1.

Hartman, D.L., A.M.G. Klein Tank, M. Rusticucci, L. Alexander, S. Brönnimann, Y. Charabi, F. Dentener, et al. 2013. "Observations: Atmosphere and Surface Supplementary Material." *Climate Change 2013 the Physical Science Basis: Working Group I Contribution to the Fifth Assessment Report of the Intergovernmental Panel on Climate Change*, 2SM-1-2SM – 30.

Howard, D. M., and P. J.A. Howard. 1993. "Relationships between CO_2 Evolution, Moisture Content and Temperature for a Range of Soil Types." *Soil Biology and Biochemistry* 25 (11): 1537–46. https://doi.org/10.1016/0038-0717(93)90008-Y.

Howard, P. J.A., and D. M. Howard. 1990. "Use of Organic Carbon and Loss-on-Ignition to Estimate Soil Organic Matter in Different Soil Types and Horizons." *Biology and Fertility of Soils* 9 (4): 306–10. https://doi.org/10.1007/BF00634106.

Iovieno, Paola, and Erland Bååth. 2008. "Effect of Drying and Rewetting on Bacterial Growth Rates in Soil." *FEMS Microbiology Ecology* 65 (3): 400–407. https://doi.org/10.1111/j.1574-6941.2008.00524.x.

IPCC, 2013: Climate Change 2013: The Physical Science Basis. Contribution of Working Group I to the Fifth Assessment Report of the Intergovernmental Panel on Climate Change [Stocker, T.F., D. Qin, G.-K. Plattner, M. Tignor, S.K. Allen, J. Boschung, A. Nauels, Y. Xia, V. Bex and P.M. Midgley (eds.)]. Cambridge University Press, Cambridge, United Kingdom and New York, NY, USA, 1535 pp.

Janssens, I. A., W. Dieleman, S. Luyssaert, J. A. Subke, M. Reichstein, R. Ceulemans, P. Ciais, et al. 2010. "Reduction of Forest Soil Respiration in Response to Nitrogen Deposition." *Nature Geoscience* 3 (5): 315–22. https://doi.org/10.1038/ngeo844.

Janssens, I.A. et al. (2003). Climatic Influences on Seasonal and Spatial Differences in Soil CO2 Efflux. In: Valentini, R. (eds) Fluxes of Carbon, Water and Energy of European Forests. Ecological Studies, vol 163. Springer, Berlin, Heidelberg. https://doi.org/10.1007/978-3-662-05171-9_12

Janssens, Ivan A, S Têtè, Reinhart Ceulemans, and Groupe De Guyane. 1998. "Soil CO_2 Efflux Rates in Different Tropical Vegetation Types in French Guiana." *Ann. Sci. For.* 55: 671–80.

Jarvis, Paul, Ana Rey, Charalampos Petsikos, Lisa Wingate, Mark Rayment, João Pereira, João Banza, et al. 2007. "Drying and Wetting of Mediterranean Soils Stimulates Decomposition and Carbon Dioxide Emission: The 'Birch Effect.'" *Tree Physiology* 27 (7): 929–40. https://doi.org/10.1093/treephys/27.7.929.

Kitzler, B., S. Zechmeister-Boltenstern, C. Holtermann, U. Skiba, and K. Butterbach-Bahl. 2006. "Nitrogen Oxides Emission from Two Beech Forests Subjected to Different Nitrogen Loads." *Biogeosciences* 3 (3): 293–310. https://doi.org/10.5194/bg-3-293-2006.

Lankreijer, H., Janssens, I.A., Buchmann, N., Longdoz, B., Epron, D., Dore, S. (2003). Measurement of Soil Respiration. In: Valentini, R. (eds) Fluxes of Carbon, Water and

Energy of European Forests. Ecological Studies, vol 163. Springer, Berlin, Heidelberg. https://doi.org/10.1007/978-3-662-05171-9_3

Law, B. E., F. M. Kelliher, D. D. Baldocchi, P. M. Anthoni, J. Irvine, D. Moore, and S. Van Tuyl. 2001. "Spatial and Temporal Variation in Respiration in a Young Ponderosa Pine Forest during a Summer Drought." *Agricultural and Forest Meteorology* 110 (1): 27–43. https://doi.org/10.1016/S0168-1923(01)00279-9.

Lawrence, Corey R., Jason C. Neff, and Joshua P. Schimel. 2009. "Does Adding Microbial Mechanisms of Decomposition Improve Soil Organic Matter Models? A Comparison of Four Models Using Data from a Pulsed Rewetting Experiment." *Soil Biology and Biochemistry* 41 (9): 1923–34. https://doi.org/10.1016/j.soilbio.2009.06.016.

Lee, K. H., and S. Jose. 2003. "Soil Respiration and Microbial Biomass in a Pecan - Cotton Alley Cropping System in Southern USA." *Agroforestry Systems* 58 (1): 45–54. https://doi.org/10.1023/A:1025404019211.

Leitner, Sonja, Peter M. Homyak, Joseph C. Blankinship, Jennifer Eberwein, G. Darrel Jenerette, Sophie Zechmeister-Boltenstern, and Joshua P. Schimel. 2017. "Linking NO and N2O Emission Pulses with the Mobilization of Mineral and Organic N upon Rewetting Dry Soils." *Soil Biology and Biochemistry* 115: 461–66. https://doi.org/10.1016/j.soilbio.2017.09.005.

Leitner, Sonja, Pia Minixhofer, Erich Inselsbacher, Katharina M. Keiblinger, Michael Zimmermann, and Sophie Zechmeister-Boltenstern. 2017. "Short-Term Soil Mineral and Organic Nitrogen Fluxes during Moderate and Severe Drying–Rewetting Events." *Applied Soil Ecology* 114: 28–33. https://doi.org/10.1016/j.apsoil.2017.02.014.

ha https://doi.org/10.1111/1365-2745.13550.

Leizeaga, Ainara, Annelein Meisner, Johannes Rousk, and Erland Bååth. 2022. "Repeated Drying and Rewetting Cycles Accelerate Bacterial Growth Recovery after Rewetting." *Biology and Fertility of Soils* 58 (4): 365–74. https://doi.org/10.1007/s00374-022-01623-2.

Lloyd, J, and J A Taylor. 1994. On the Temperature Dependence of Soil Respiration (3): 315–23.

Luo, G. J., N. Brüggemann, B. Wolf, R. Gasche, R. Grote, and K. Butterbach-Bahl. 2012. "Decadal Variability of Soil CO_2, NO, N_2O, and CH_4 fluxes at the Höglwald Forest, Germany." *Biogeosciences* 9 (5): 1741–63. https://doi.org/10.5194/bg-9-1741-2012.

Manzoni, S., S. M. Schaeffer, G. Katul, A. Porporato, and J. P. Schimel. 2014. "A Theoretical Analysis of Microbial Eco-Physiological and Diffusion Limitations to Carbon Cycling in Drying Soils." *Soil Biology and Biochemistry* 73: 69–83. https://doi.org/10.1016/j.soilbio.2014.02.008.

Meisner, Annelein, Johannes Rousk, and Erland Bååth. 2015. "Prolonged Drought Changes the Bacterial Growth Response to Rewetting." *Soil Biology and Biochemistry* 88: 314–22. https://doi.org/10.1016/j.soilbio.2015.06.002.

Miller, Amy E., Joshua P. Schimel, Thomas Meixner, James O. Sickman, and John M. Melack. 2005. “Episodic Rewetting Enhances Carbon and Nitrogen Release from Chaparral Soils.” *Soil Biology and Biochemistry* 37 (12): 2195–2204. https://doi.org/10.1016/j.soilbio.2005.03.021.

Moyano, F. E., N. Vasilyeva, L. Bouckaert, F. Cook, J. Craine, J. Curiel Yuste, A. Don, et al. 2012. “The Moisture Response of Soil Heterotrophic Respiration: Interaction with Soil Properties.” *Biogeosciences* 9 (3): 1173–82. https://doi.org/10.5194/bg-9-1173-2012.

Moyano, Fernando E., Stefano Manzoni, and Claire Chenu. 2013. “Responses of Soil Heterotrophic Respiration to Moisture Availability: An Exploration of Processes and Models.” *Soil Biology and Biochemistry* 59: 72–85. https://doi.org/10.1016/j.soilbio.2013.01.002.

Navarro-García, Federico, Miguel Ángel Casermeiro, and Joshua P. Schimel. 2012. “When Structure Means Conservation: Effect of Aggregate Structure in Controlling Microbial Responses to Rewetting Events.” *Soil Biology and Biochemistry* 44 (1): 1–8. https://doi.org/10.1016/j.soilbio.2011.09.019.

Orth, René, Jakob Zscheischler, and Sonia I. Seneviratne. 2016. “Record Dry Summer in 2015 Challenges Precipitation Projections in Central Europe.” *Scientific Reports* 6 (June): 1–8. https://doi.org/10.1038/srep28334.

Pan, Yude, Richard A. Birdsey, Jingyun Fang, Richard Houghton, Pekka E. Kauppi, Werner A. Kurz, Oliver L. Phillips, et al. 2011. “A Large and Persistent Carbon Sink in the World’s Forests.” *Science* 333 (6045): 988–93. https://doi.org/10.1126/science.1201609.

Parkin, T.B. and Venterea, R.T. 2010. Sampling Protocols. Chapter 3. Chamber-Based Trace Gas Flux Measurements. IN Sampling Protocols. R.F. Follett, editor. p. 3-1 to 3-39. Available at: www.ars.usda.gov/research/GRACEnet

Placella, Sarah A., Eoin L. Brodie, and Mary K. Firestone. 2012. “Rainfall-Induced Carbon Dioxide Pulses Result from Sequential Resuscitation of Phylogenetically Clustered Microbial Groups.” *Proceedings of the National Academy of Sciences of the United States of America* 109 (27): 10931–36. https://doi.org/10.1073/pnas.1204306109.

Pregitzer, Kurt S., Andrew J. Burton, Donald R. Zak, and Alan F. Talhelm. 2008. “Simulated Chronic Nitrogen Deposition Increases Carbon Storage in Northern Temperate Forests.” *Global Change Biology* 14 (1): 142–53. https://doi.org/10.1111/j.1365-2486.2007.01465.x.

Rasmussen, Craig, Katherine Heckman, William R. Wieder, Marco Keiluweit, Corey R. Lawrence, Asmeret Asefaw Berhe, Joseph C. Blankinship, et al. 2018. “Beyond Clay: Towards an Improved Set of Variables for Predicting Soil Organic Matter Content.” *Biogeochemistry* 137 (3): 297–306. https://doi.org/10.1007/s10533-018-0424-3.

Rayment, M. B., and P. G. Jarvis. 2000. “Temporal and Spatial Variation of Soil CO2 Efflux in a Canadian Boreal Forest.” *Soil Biology and Biochemistry* 32 (1): 35–45. https://doi.org/10.1016/S0038-0717(99)00110-8.

Reich, Peter B. 2010. “The Carbon Dioxide Exchange.” *Science* 329 (5993): 774–75. https://doi.org/10.1126/science.1194353.

Sawada, Kozue, Shinya Funakawa, and Takashi Kosaki. 2017. “Effect of Repeated Drying–Rewetting Cycles on Microbial Biomass Carbon in Soils with Different Climatic Histories.” *Applied Soil Ecology* 120 (February): 1–7. https://doi.org/10.1016/j.apsoil.2017.07.023.

Schimel, Joshua P., Jay M. Gulledge, Joy S. Clein-Curley, Jon E. Lindstrom, and Joan F. Braddock. 1999. “Moisture Effects on Microbial Activity and Community Structure in Decomposing Birch Litter in the Alaskan Taiga.” *Soil Biology and Biochemistry* 31 (6): 831–38. https://doi.org/10.1016/S0038-0717(98)00182-5.

Schneider, Thomas, Katharina M. Keiblinger, Emanuel Schmid, Katja Sterflinger-Gleixner, Günther Ellersdorfer, Bernd Roschitzki, Andreas Richter, Leo Eberl, Sophie Zechmeister-Boltenstern, and Kathrin Riedel. 2012. “Who Is Who in Litter Decomposition Metaproteomics Reveals Major Microbial Players and Their Biogeochemical Functions.” *ISME Journal* 6 (9): 1749–62. https://doi.org/10.1038/ismej.2012.11.

Sherwood, Steven, and Qiang Fu. 2014. “A Drier Future?” *Science* 343 (6172): 737–39. https://doi.org/10.1126/science.1247620.

Six, J., H. Bossuyt, S. Degryze, and K. Denef. 2004. “A History of Research on the Link between (Micro)Aggregates, Soil Biota, and Soil Organic Matter Dynamics.” *Soil and Tillage Research* 79 (1): 7–31. https://doi.org/10.1016/j.still.2004.03.008.

Skopp, J., M. D. Jawson, and J. W. Doran. 1990. “Steady-State Aerobic Microbial Activity as a Function of Soil Water Content.” *Soil Science Society of America Journal* 54 (6): 1619–25. https://doi.org/10.2136/sssaj1990.03615995005400060018x.

Søe, Astrid R.B., and Nina Buchmann. 2005. “Spatial and Temporal Variations in Soil Respiration in Relation to Stand Structure and Soil Parameters in an Unmanaged Beech Forest.” *Tree Physiology* 25 (11): 1427–36. https://doi.org/10.1093/treephys/25.11.1427.

Sutton, Mark A, Clare M Howard, Jan Willem Erisman, Gilles Billen, and Albert Bleeker. 2011. “The European Nitrogen Assessment: Front Matter.” *The European Nitrogen Assessment*.

Valentini, Riccardo. 2003. *Fluxes of Carbon, Water and Energy of European Forests*. https://doi.org/10.1007/978-3-662-05171-9_10.

Gestel, Natasja Van, Zheng Shi, Kees Jan Van Groenigen, Craig W. Osenberg, Louise C. Andresen, Jeffrey S. Dukes, Mark J. Hovenden, et al. 2018. “Predicting Soil Carbon Loss with Warming.” *Nature* 554 (7693): E4–5. https://doi.org/10.1038/nature25745.

Vincent, Gaëlle, Ali Reza Shahriari, Eric Lucot, Pierre Marie Badot, and Daniel Epron. 2006. “Spatial and Seasonal Variations in Soil Respiration in a Temperate Deciduous Forest with Fluctuating Water Table.” *Soil Biology and Biochemistry* 38 (9): 2527–35. https://doi.org/10.1016/j.soilbio.2006.03.009.

Williams, Mark A., and Kang Xia. 2009. “Characterization of the Water Soluble Soil Organic Pool Following the Rewetting of Dry Soil in a Drought-Prone Tallgrass Prairie.” *Soil Biology and Biochemistry* 41 (1): 21–28. https://doi.org/10.1016/j.soilbio.2008.08.013.

Xiang, Shu Rong, Allen Doyle, Patricia A. Holden, and Joshua P. Schimel. 2008. “Drying and Rewetting Effects on C and N Mineralization and Microbial Activity in Surface and Subsurface California Grassland Soils.” *Soil Biology and Biochemistry* 40 (9): 2281–89. https://doi.org/10.1016/j.soilbio.2008.05.004.

Xu, Ming, and Hua Shang. 2016. “Contribution of Soil Respiration to the Global Carbon Equation.” *Journal of Plant Physiology* 203: 16–28. https://doi.org/10.1016/j.jplph.2016.08.007.

Zaehle, Sönke, and Daniela Dalmonech. 2011. “Carbon-Nitrogen Interactions on Land at Global Scales: Current Understanding in Modelling Climate Biosphere Feedbacks.” *Current Opinion in Environmental Sustainability* 3 (5): 311–20. https://doi.org/10.1016/j.cosust.2011.08.008.

Zhao, Bingzi, Ji Chen, Jiabao Zhang, and Shengwu Qin. 2010. “Soil Microbial Biomass and Activity Response to Repeated Drying-Rewetting Cycles along a Soil Fertility Gradient Modified by Long-Term Fertilization Management Practices.” *Geoderma* 160 (2): 218–24. https://doi.org/10.1016/j.geoderma.2010.09.024.

Zhong, Yangquanwei, Weiming Yan, and Zhouping Shangguan. 2016. “The Effects of Nitrogen Enrichment on Soil CO2 Fluxes Depending on Temperature and Soil Properties.” *Global Ecology and Biogeography* 25 (4): 475–88. https://doi.org/10.1111/geb.12430.

Zhou, Lingyan, Xuhui Zhou, Baocheng Zhang, Meng Lu, Yiqi Luo, Lingli Liu, and Bo Li. 2014. “Different Responses of Soil Respiration and Its Components to Nitrogen Addition among Biomes: A Meta-Analysis.” *Global Change Biology* 20 (7): 2332–43. https://doi.org/10.1111/gcb.12490.

List of tables / figures

Figure 2-1. Timeplan of the year 2021 at Klausen-Leopoldsdorf research site. Adapted from Institute of Soil Research, BOKU. 9
Figure 2-2. Experimental setup at Klausen-Leopoldsdorf research site. Each of the 16 squared plots (3 m x 3 m; red squares), was equiped with an automated chamber (black squares) connected to a "Gas Flux Trailer" (grey rectangle). Half of the plots were covered with rain-out shelters (green dashed rectangles) since May 4th, 2021. The plots were randomly assigned and equally distributed to each of the four treatments resulted. Plots number 1, 5, 10, and 13 were assigned to Control (C) treatment; 2, 6, 9, and 14 to Control with N addition (C+N); 3, 7, 11, and 15 to Severe DRW stress (S); 4, 8, 12, and 16 to Severe DRW stress with N addition (S+N). Source: Institute of Soil Research, BOKU. 10
Figure 2-3. Evolution of daily averages for soil water content (%) (left axis) and water inputs (mm) (right axis) between June 1st and November 12th. The soil water content is differentiated by DRW (dashed line) and control (continued line) plots. The water inputs are differentiated by precipitation (black columns) and irrigation (dashed columns). The data analysed in the current thesis falls between the red lines. 13
Figure 2-4. Evolution of daily averages for soil water content (%) (left axis) and water inputs (mm) (right axis) between August 19th and September 15th. The soil water content is differentiated by DRW (dashed line) and control (continued line) plots. The water inputs are differentiated by precipitation (solid columns) and irrigation (dotted columns). 14
Figure 2-5. Evolution of daily averaged temperature between August 19th and September 15th, at 5 cm soil depth in control (solid line) and DRW stress (dashed line), and air temperature at 2 m above soil (dashed and pointed line). "drought" is referring to "DRW stress". 14
Figure 3-1. Boxplots of daily average soil efflux (CO_2-C m^{-2} h^{-1}) from each plot, and coloured by the 4 treatments combination. Boxplots contain only data from August 24th and 31st. 16
Figure 3-2. Boxplots of daily average soil efflux (CO_2-C m^{-2} h^{-1}) from each plot and coloured by the 4 treatments combination. The data for the full period (28 days) is included. The points in black are all the flux observations (28). 18
Figure 3-3. Time series of daily averaged soil CO_2 emission [mg CO_2-C m^{-2} h^{-1}], per treatment and including nitrogen addition levels, for the 28 days between August 19th and September 15th. Error bars indicate SE. 19
Figure 3-4. Time series of daily averaged soil CO_2 emission [mg CO_2-C m^{-2} h^{-1}] (left axis) and soil water content [m^3 m^{-3}] (right axis), and precipitation/irrigation [mm] (left axis) for the 28 days between August 19th and September 15th, and considering only the rainfall manipulation (pooled and averaged into Average All S and C). Error bars indicate SE. 20
Figure 3-5. Contour map of soil fluxes driven by soil temperature and soil water content in the control treatment. Elaborated with Surfer® (Golden Software, LLC). 23
Figure 3-6. Contour map of soil fluxes driven by soil temperature and soil water content in drought treatment. Elaborated with Surfer® (Golden Software, LLC). "Drought" stands for "DRW stress" treatment. 23

Figure 3-7. Contour map of soil fluxes driven by soil temperature and soil water content in all observations, control and drought treatments combined. Elaborated with Surfer® (Golden Software, LLC). “Drought” stands for “DRW stress” treatment. 24
Figure 0-1. Scatterplot of soil efflux (mg CO_2-C m^{-2} h^{-1}) against soil moisture. “All C” referers to averaged in control plots while “All S” corresponds to “DRW stress”. The dashed line results from the automated curve fitting function in Microsoft Excel. 1
Figure 0-2. Scatterplot of soil efflux (mg CO_2-C m^{-2} h^{-1}) against soil temperature. “All C” referers to averaged in control plots while “All S” corresponds to “DRW stress”. The dashed line resulted from the automated curve fitting function in Microsoft Excel.....1
Figure 0-3. Ratio soil CO_2 efflux DRW:Control (ratio efflux s/c) plotted against the ratio soil moisture DRW:Control (ratio moist s/c). There is an abrupt change in ratio efflux s/c around a value of ratio moist s/c around 0.7, which can indicate a decoupling between soil CO_2 efflux and the soil moisture content. Idea extracted from other work (missing reference) and adapted to the current thesis data. A polinomial curve was fitted used Microsoft Excel curve estimation. 2

Table 2-1. Main features of site Klausen-Leopoldsdorf. Data based on Kitzler et al. (2006). 8
Table 3-1. Soil parameters mean and SD. Rho Spearman's correlation and R^2 linear regression were calculated, relating the variables with the log-transformed (log_{10}) CO_2 efflux. Significance: * = P<0.05; ** = P<0.01. Transformation of the explanatory variables is indicated. Abbreviations: dw = soil dry weight; SD = standard deviation. 17
Table 3-2. Mean +- SE (min-max) of averaged CO_2 fluxes along days of the four treatments when including N addition levels. Three periods were considered, complete (28 days from August 19th to September 15th), before rewetting (6 days from August 19th to 24th), and after rewetting (22 days from August 25th to September 15th). The p-values inform the Kruskal-Wallis test. The letters above the means indicate ranks from Wilcoxon's sum rank test with Bonferroni correction. 18
Table 3-3. Mean +- SE (min-max) of averaged CO_2 fluxes [mg CO_2-C m^{-2} h^{-1}] along days of the two levels of the rainfall manipulation. Three periods were considered, complete (28 days from August 19th to September 15th), before rewetting (6 days from August 19th to 24th), and after rewetting (22 days from August 25th to September 15th). The p-values inform Welch's test results. 20
Table 3-4. Mean +- SE (min-max) of the daily mean soil temperature at 5 cm depth [°C] for "control" and "drought" plots averaged and differentiated by period. Three periods were considered, complete (28 days from August 19th to September 15th), before rewetting (6 days from August 19th to 24th), and after rewetting (22 days from August 25th to September 15th). The p-values inform Student's t-test results. 21
Table 3-5. Mean +- SE (min-max) of daily mean soil water content at 15 cm depth [%] for "control" and "drought" plots averaged and differentiated by period. Three periods were considered, complete (28 days from August 19th to September 15th), before rewetting (6 days from August 19th to 24th), and after rewetting (22 days from August 25th to September 15th). The p-values inform Welch's t-test results. 21
Table 3-6. Simple and multiple regression analysis between mean daily CO_2 fluxes against soil temperature and moisture. Pearson's R^2 was informed. Significance: * p<0.05, ** p<0.01, *** p<0.001. 22
Table 0-1. Mean ± SE (min-max) of soil microbial biomass carbon [C mg (soil kg)$^{-1}$] and nitrogen [N mg (soil kg)$^{-1}$], dissolved organic carbon [C mg (soil kg)$^{-1}$] and nitrogen [N mg (soil kg)$^{-1}$], nitrate [µg NO_3^--N (g dw)$^{-1}$], and ammonium [µg NH_4^+-N (g dry weight)$^{-1}$] for "control" and "DRW stress" plots averaged across plots and differentiated by periods and depths (10 and 20 cm). The two sampling dates were August 24th and 31st, but in the table they are called before and after rewetting, respectively. The p-values informed the results of Kruskall-Wallis tests when the number of mean comparisons was four and Welch's or Student's t tests when it was two, and depending on the variance. Letters in superscript specify the rank by Wilcoxon's rank sum test with Bonferroni correction. 1

Appendix A: Supplementary data

Table 0-1. Mean ± SE (min-max) of soil microbial biomass carbon [C mg (soil kg)$^{-1}$] and nitrogen [N mg (soil kg)$^{-1}$], dissolved organic carbon [C mg (soil kg)$^{-1}$] and nitrogen [N mg (soil kg)$^{-1}$], nitrate [µg NO_3^--N (g dw)$^{-1}$], and ammonium [µg NH_4^+-N (g dry weight)$^{-1}$] for "control" and "DRW stress" plots averaged across plots and differentiated by periods and depths (10 and 20 cm). The two sampling dates were August 24th and 31st, but in the table they are called before and after rewetting, respectively. The p-values informed the results of Kruskall-Wallis tests when the number of mean comparisons was four and Welch's or Student's t tests when it was two, and depending on the variance. Letters in superscript specify the rank by Wilcoxon's rank sum test with Bonferroni correction.

	Precipitation exclusion			Prec. Exc. + Nitrogen addition				
parameter	**control**	**DRW stress**	***p-value***	**c**	**c + n**	**s**	**s + n**	***p-value***
sand [%] (10 cm)	14.22 ± 1.47 (10.17-23.47)	12.48 ± 0.93 (9.21-17.07)	*0.33*	15.76 ± 2.63 (12.37-23.47)	12.69 ± 1.26 (10.17-16.19)	13.86 ± 1.51 (9.91-17.07)	11.11 ± 0.71 (9.21-12.40)	*0.3*
sand [%] (20 cm)	11.17 ± 0.76 (8.59-15.97)	10.64 ± 0.60 (8.85-13.28)	*0.59*	12.32 ± 1.23 (10.86-15.97)	10.03 ± 0.59 (8.59-11.29)	11.07 ± 1.12 (8.94-13.28)	10.22 ± 0.56 (8.85-11.57)	*0.33*
silt [%] (10 cm)	55.32 ± 1.62 (51.89-62.69)	55.13 ± 1.61 (47.22-60.06)	*0.93*	52.54 ± 0.22 (51.89-52.80)	58.10 ± 2.66 (52.04-62.69)	54.34 ± 1.69 (50.65-57.70)	55.92 ± 2.96 (47.22-60.06)	*0.36*
silt [%] (20 cm)	52.96 ± 0.73 (49.27-56.51)	55.74 ± 1.15 (51.23-60.00)	*0.061*	52.01 ± 1.00 (49.25-53.85)	53.92 ± 0.95 (51.98-56.51)	55.22 ± 1.61 (52.66-59.87)	56.26 ± 1.84 (51.23-60.00)	*0.22*
clay [%] (10 cm)	30.4 ± 1.58 (23.73-35.73)	32.39 ± 1.31 (28.78-40.38)	*0.36*	31.7 ± 2.75 (23.73-35.73)	29.21 ± 1.76 (25.18-32.53)	31.8 ± 1.30 (28.78-34.43)	32.98 ± 2.48 (29.88-40.38)	*0.66*
clay [%] (20 cm)	35.86 ± 1.04 (30.18-39.78)	33.62 ± 0.98 (30.78-38.4)	*0.14*	35.68 ± 2.00 (30.18-39.78)	36.05 ± 1.01 (33.88-38.1)	33.71 ± 1.67 (30.78-38.4)	33.53 ± 1.29 (31.15-37.2)	*0.56*
clay [%] (20 cm)	3.27 ± 0.21 (2.53-4.17)	3.85 ± 0.31 (2.91-5.56)	*0.14*	3.14 ± 0.35 (2.53-3.79)	3.40 ± 0.27 (3.03-4.17)	4.08 ± 0.52 (3.16-5.56)	3.63 ± 0.36 (2.91-4.53)	*0.41*
Total carbon [w/w%] (20 cm)	2.09 ± 0.23 (1.26-3.36)	2.70 ± 0.34 (1.60-4.35)	*0.16*	2.09 ± 0.47 (1.26-3.36)	2.09 ± 0.17 (1.82-2.54)	2.73 ± 0.41 (1.60-3.46)	2.67 ± 0.60 (1.64-4.35)	*0.6*
Total nitrogen [w/w%] (10 cm)	0.17 ± 0.01 (0.1-0.21)	0.20 ± 0.02 (0.14-0.26)	*0.19*	0.16 ± 0.02 (0.1-0.19)	0.19 ± 0.02 (0.15-0.21)	0.22 ± 0.03 (0.14-0.26)	0.19 ± 0.02 (0.15-0.23)	*0.26*

	Total nitrogen [w/w%] (20 cm)	0.10 ± 0.01 (0.06-0.17)	0.15 ± 0.02 (0.07-0.22)	***0.04***	0.1 ± 0.03 (0.06-0.17)	0.1 ± 0.01 (0.08-0.12)	0.17 ± 0.03 (0.1-0.22)	0.13 ± 0.03 (0.07-0.21)	*0.16*
	C:N 10 cm	19.44 ± 1.36 (14.85-26.26)	19.27 ± 1.00 (15.27-22.38)	*0.92*	20.81 ± 2.22 (15.50-26.26)	18.06 ± 1.58 (14.85-20.78)	18.84 ± 1.91 (15.27-22.38)	17.70 ± 0.93 (17.60-22.04)	*0.71*
	C:N 20 cm	21.92 ± 1.16 (17.80-27.33)	18.21 ± 1.07 (15.37-24.50)	***0.04***	[ab]21.56 ± 1.34 (19.52-25.22)	[a]22.28 ± 2.09 (17.80-27.33)	[c]16.10 ± 0.34 (15.37-17.02)	[bc]20.33 ± 1.51 (18.12-24.50)	***0.04***
before rewett.	*microbial biomass carbon [C mg (soil kg)$^{-1}$] (10 cm)*	185.23 ± 14.44 (117.82-233.80)	142.19 ± 15.43 (79.17-209.5)	*0.06*	174.31 ± 24.04 (117.82-233.8)	196.16 ± 17.76 (146.38-227.2)	137.04 ± 30.3 (79.17-209.5)	147.34 ± 13.24 (108.25-163.71)	*0.28*
after rewett.		131.55 ± 12.91 (67.21-197.25)	119.61 ± 9.18 (98.35-176.54)	*0.79*	128.86 ± 26.78 (67.21-197.25)	134.24 ± 7.50 (120.31-153.39)	128.03 ± 18.05 (98.35-176.54)	111.18 ± 4.53 (101.50-119.80)	*0.46*
p-value		***0.015***	*0.23*		*0.25*	*0.03*	*0.81*	*0.066*	
before rewett.	*microbial biomass carbon [C mg (soil kg)$^{-1}$] (20 cm)*	167.68 ± 27.76 (86.18-290.4)	170.92 ± 33.13 (62.64-349.13)	*0.94*	169.17 ±42.06 (110.22-290.4)	166.18 ± 42.72 (86.18-286.68)	161.32 ± 33.54 (98.26-255.58)	180.52 ± 62.75 (62.64-349.13)	*0.99*
after rewett.		116.63 ± 18.20 (65.25-213.94)	123.08 ± 9.74 (88.31-169.72)	*0.76*	120.53 ± 33.58 (65.25-213.94)	112.74 ± 20.18 (81.85-171.23)	130.69 ± 17.11 (94.12-169.72)	115.47 ± 10.55 (88.31-136.55)	*0.94*
p-value		*0.15*	*0.2*		*0.4*	*0.32*	*0.46*	*0.38*	
before rewett.	*microbial biomass nitrogen [N mg (soil kg)$^{-1}$] (10 cm)*	24.36 ± 2.22 (17.0-33.88)	15.44 ± 2.34 (7.64-24.89)	***0.015***	23.58 ± 3.9 (17.0-33.88)	25.13 ± 2.75 (17.03-29.19)	15.81 ± 3.99 (7.64-24.89)	15.08 ± 3.08 (8.08-20.61)	*0.136*
after rewett.		18.60 ± 1.31 (11.61-22.72)	18.34 ± 1.72 (12.19-26.11)	*0.9*	17.67 ± 2.32 (11.61-22.72)	19.53 ± 1.43 (15.30-21.48)	19.57 ± 3.26 (12.19-26.11)	17.11 ± 1.46 (13.43-20.54)	*0.81*
p-value		***0.047***	*0.34*		*0.25*	*0.14*	*0.49*	*0.58*	
before rewett.	*microbial biomass nitrogen [N mg (soil kg)$^{-1}$] (20 cm)*	22.94 ± 4.25 (11.73-48.15)	19.54 ± 4.31 (5.35-44.58)	*0.58*	25.1 ± 7.95 (13.36-48.15)	20.78 ± 4.25 (11.73-31.88)	18.0 ± 3.21 (12.79-27.02)	21.06 ± 8.65 (5.35-44.58)	*0.89*
after rewett.		16.59 ± 1.47 (9.8±23.06)	21.86 ± 2.77 (14.31-37.42)	*0.12*	17.07 ± 2.81 (9.86-23.06)	16.11 ± 1.41 (13.23-18.95)	24.00 ± 5.26 (14.62-37.42)	19.71 ± 2.28 (14.31-25.42)	*0.36*
p-value		*0.19*	*0.66*		*0.4*	*0.36*	*0.38*	*0.89*	

before rewett.	*dissolved organic carbon [C mg (soil kg)$^{-1}$] (10 cm)*	197.97 ± 13.83 (135.56-251.45)	216.72 ± 11.83 (184.35-289.62)	*0.89*	175.68 ± 17.15 (135.56-219.29)	220.27 ± 16.35 (187.89-251.45)	203.84 ± 11.83 (184.35-236.87)	229.6 ± 20.05 (205.77-289.62)	*0.32*
after rewett.		205.32 ± 16.28 (127.55-267.55)	210.86 ± 8.33 (175.64-245.12)	*0.77*	192.64 ± 27.97 (127.5-244.5)	217.99 ± 18.62 (181.46-267.55)	215.31 ± 14.52 (175.64-245.12)	206.41 ± 10.00 (181.29-229.20)	*0.78*
p-value		*0.74*	*0.69*		*0.63*	*0.93*	*0.56*	*0.35*	
before rewett.	*dissolved organic carbon [C mg (soil kg)$^{-1}$] (20 cm)*	175.66 ± 12.65 (133.25-239.36)	206.41 ± 17.2 (150.56-280.73)	*0.17*	160.78 ± 14.98 (133.25-201.26)	190.54 ± 19.35 (154.93-239.36)	176.49 ± 8.83 (150.56-188.42)	236.33 ± 26.6 (172.5-280.73)	*0.069*
after rewett.		169.47 ± 12.45 (128.01-213.66)	192.33 ± 10.50 (163.83-249.19)	*0.18*	165.58 ± 21.50 (128.01-205.16)	173.36 ± 15.79 (147.23-213.66)	194.77 ± 10.68 (165.13-215.19)	189.89 ± 19.90 (163.83-249.19)	*0.62*
p-value		*0.73*	*0.5*		*0.86*	*0.52*	*0.24*	*0.22*	
before rewett.	*dissolved organic nitrogen [N mg (soil kg)$^{-1}$] (10 cm)*	23.24 ± 1.95 (14.22-33.1)	25.5 ± 1.42 (19.53-31.47)	*0.37*	22.71 ± 3.91 (14.22-33.1)	24.78 ± 1.52 (20.08-27.17)	26.68 ± 2.51 (19.53-31.47)	26.31 ± 1.64 (23.15-30.74)	*0.79*
after rewett.		24.78 ± 1.65 (15.82-30.82)	30.00 ± 2.31 (21.17-40.71)	*0.086*	23.25 ± 3.18 (15.82-30.82)	26.30 ± 1.00 (24.71-28.94)	31.64 ± 4.08 (21.17-40.71)	28.36 ± 2.51 (23.97-35.36)	*0.275*
p-value		*0.56*	*0.12*		*0.92*	*0.22*	*0.21*	*0.52*	
before rewett.	*dissolved organic nitrogen [N mg (soil kg)$^{-1}$] (20 cm)*	21.73 ± 1.14 (15.74-25.54)	24.44 ± 1.78 (17.81-33.64)	*0.22*	20.64 ± 2.11 (15.74-25.54)	22.81 ± 0.93 (20.7-24.67)	22.15 ± 2.07 (17.81-26.29)	26.73 ± 2.62 (22.33-33.64)	*0.23*
after rewett.		21.14 ± 1.84 (15.16-30.73)	24.03 ± 1.49 (19.55-31.15)	*0.24*	19.31 ± 2.48 (15.16-25.93)	22.97 ± 2.72 (18.68-30.73)	24.02 ± 2.08 (19.55-28.89)	24.05 ± 2.46 (20.24-31.15)	*0.5*
p-value		*0.79*	*0.86*		*0.7*	*0.96*	*0.55*	*0.49*	
before rewett.	*nitrate [µg NO_3^--N (g dry weight)$^{-1}$] (10 cm)*	3.05 ± 1.18 (0.38-9.87)	3.22 ± 0.62 (1.10-5.95)	*0.9*	3.00 ± 2.30 (0.38-9.87)	3.10 ± 1.08 (1.52-6.15)	1.85 ± 0.44 (1.10-3.13)	4.59 ± 0.60 (3.13-5.95)	*0.56*
after rewett.		1.59 ± 0.46 (0.11-3.68)	2.55 ± 0.63 (0.11-5.59)	*0.23*	1.58 ± 0.53 (0.55-2.88)	1.60 ± 0.83 (0.11-3.68)	2.22 ± 0.53 (0.86-3.45)	2.91 ± 1.22 (0.11-5.59)	*0.64*
p-value		*0.28*	*0.47*		*0.59*	*0.31*	*0.61*	*0.28*	

before rewett.	*nitrate [µg NO_3^--N (g dry weight)$^{-1}$] (20 cm)*	1.67 ± 0.34 (0.56-3.52)	1.68 ± 0.32 (0.76-3.54)	*0.98*	1.52 ± 0.38 (0.86-2.54)	1.82 ± 0.62 (0.56-3.52)	1.28 ± 0.18 (0.87-1.68)	2.09 ± 0.59 (0.76-3.54)	*0.66*
after rewett.		1.36 ± 0.31 (0.22-3.33)	1.08 ± 0.12 (0.63-1.77)	*0.42*	0.89 ± 0.24 (0.22-1.22)	1.84 ± 0.50 (1.22-3.33)	1.33 ± 0.15 (1.16-1.77)	0.84 ± 0.08 (0.63-0.99)	*0.1*
p-value		*0.52*	*0.12*		*0.22*	*0.98*	*0.83*	*0.12*	
before rewett.	*ammonium [µg NH_4^+-N (g dry weight)$^{-1}$] (10 cm)*	7.05 ± 1.31 (3.27-15.71)	7.04 ± 0.51 (4.51-8.92)	*0.99*	8.48 ± 2.45 (4.94-15.71)	5.63 ± 0.83 (3.27-7.02)	7.20 ± 0.37 (6.26-7.87)	6.88 ± 1.04 (4.51-8.92)	*0.57*
after rewett.		5.93 ± 0.85 (3.21-11.07)	8.94 ± 1.11 (5.07-15.17)	***0.0495***	5.08 ± 0.76 (3.21-6.40)	6.78 ± 1.53 (4.26-11.07)	10.08 ± 1.70 (8.13-15.17)	7.80 ± 1.42 (5.07-11.76)	*0.14*
p-value		*0.49*	*0.15*		*0.26*	*0.54*	*0.16*	*0.62*	
before rewett.	*ammonium [µg NH_4^+-N (g dry weight)$^{-1}$] (20 cm)*	6.14 ± 0.53 (3.90-8.68)	5.76 ± 0.46 (4.16-7.19)	*0.59*	6.28 ± 0.99 (3.90-8.68)	6.01 ± 0.56 (4.92-7.49)	5.58 ± 0.71 (4.16-7.06)	5.93 ± 0.68 (4.18-7.19)	*0.93*
after rewett.		5.38 ± 0.98 (2.23-11.47)	5.28 ± 0.42 (3.83-7.29)	*0.93*	3.97 ± 0.65 (2.23-5.19)	6.79 ± 1.66 (3.68-11.47)	5.38 ± 0.50 (4.03-6.32)	5.17 ± 0.75 (3.83-7.29)	*0.31*
p-value		*0.51*	*0.46*		*0.11*	*0.68*	*0.83*	*0.48*	

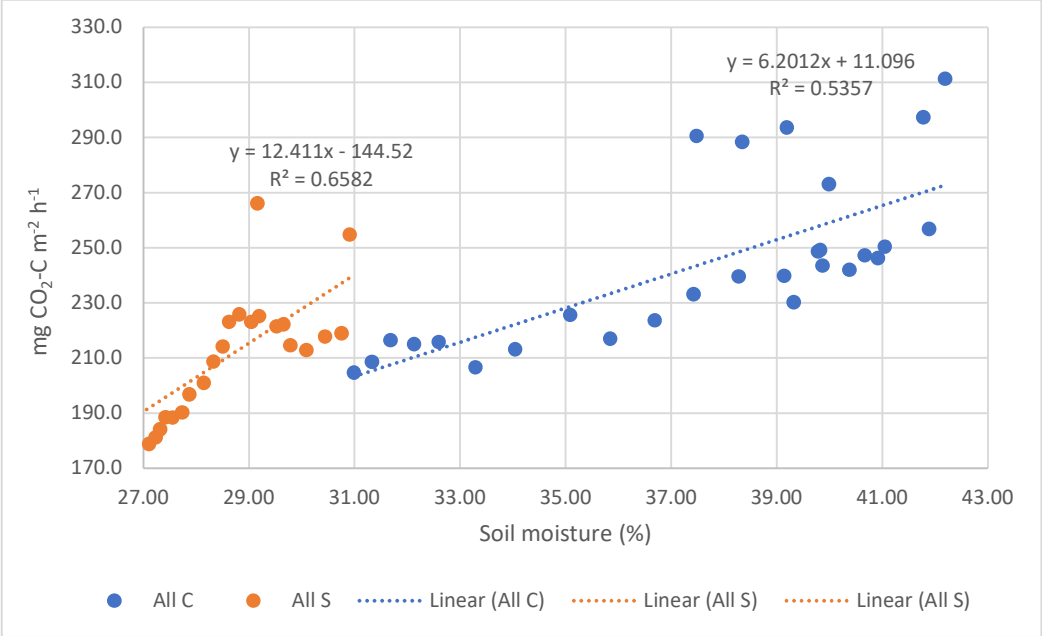

Figure 0-1. Scatterplot of soil efflux (mg CO_2-C m^{-2} h^{-1}) against soil moisture. "All C" refers to average in control plots while "All S" corresponds to "DRW stress". The dashed line results from the automated curve fitting function in Microsoft Excel.

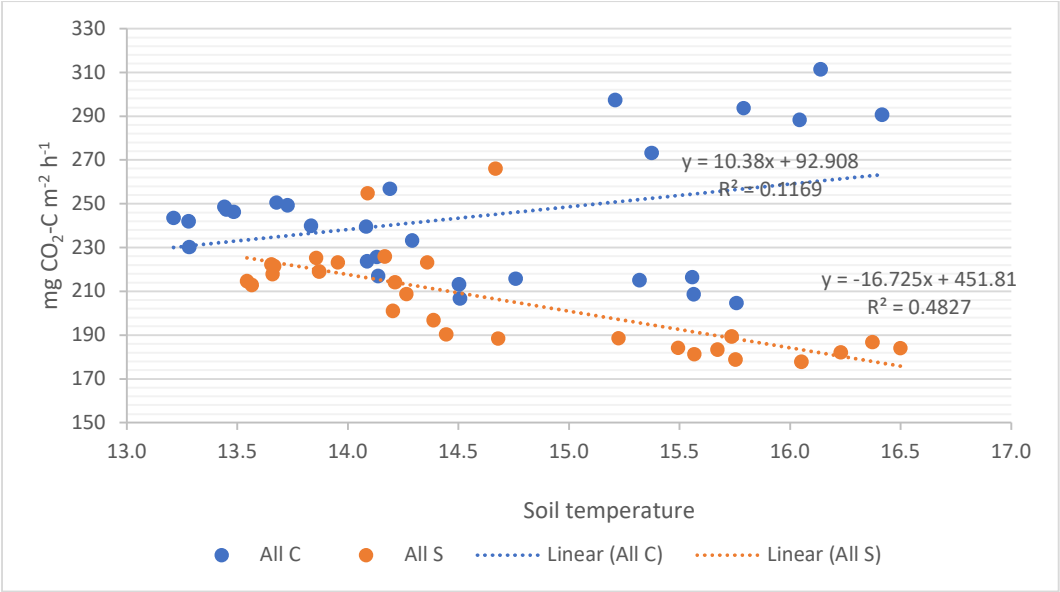

Figure 0-2. Scatterplot of soil efflux (mg CO_2-C m^{-2} h^{-1}) against soil temperature. "All C" referers to averaged in control plots while "All S" corresponds to "DRW stress". The dashed line resulted from the automated curve fitting function in Microsoft Excel.

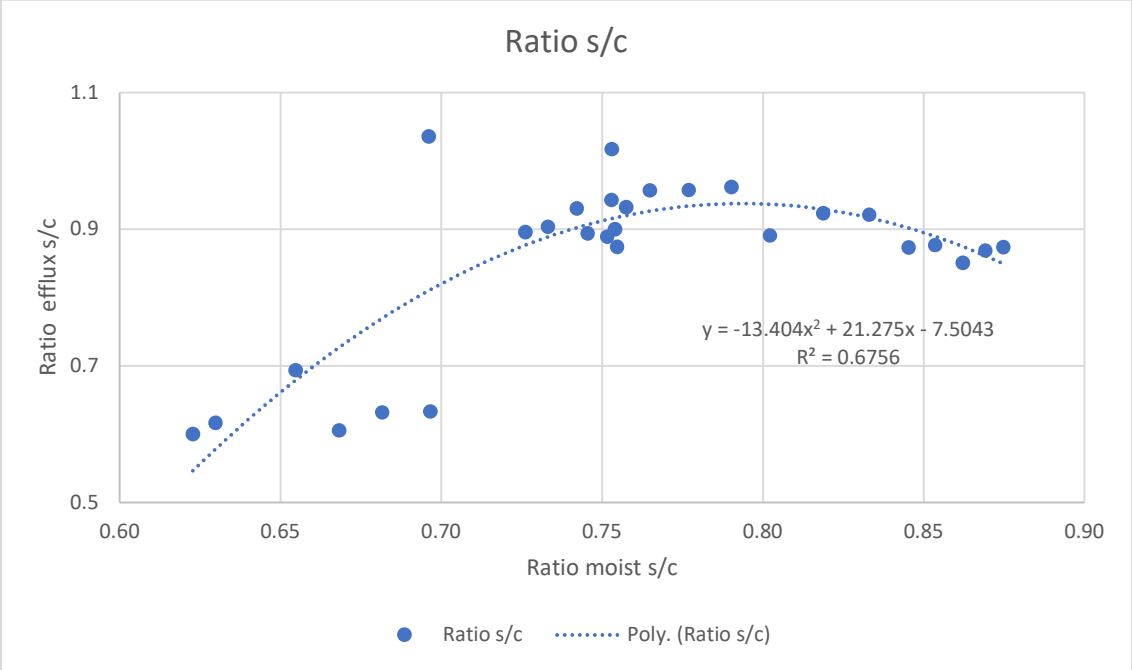

Figure 0-3. Ratio soil CO_2 efflux DRW:Control (ratio efflux s/c) plotted against the ratio soil moisture DRW:Control (ratio moist s/c). There is an abrupt change in ratio efflux s/c around a value of ratio moist s/c around 0.7, which can indicate a decoupling between soil CO_2 efflux and the soil moisture content. Idea extracted from other work (missing reference) and adapted to the current thesis data. A polinomial curve was fitted used Microsoft Excel curve estimation.